Multilepton signals from supersymmetry at hadron supercolliders

Howard Baer
Physics Department, Florida State University, Tallahassee, Florida 32306

Xerxes Tata
Department of Physics and Astronomy, University of Hawaii, Honolulu, Hawaii 96822

Jeffrey Woodside
Department of Physics and Ames Laboratory, Iowa State University, Ames, Iowa 50011
(Received 7 August 1991)

We have developed a new event generator SUSYSM to simulate the production of squarks and gluinos at hadron supercolliders including all the cascade decays as given by the minimal supersymmetric model. The simulation incorporates final-state hadronization and fragmentation effects for the decays of heavy flavors. We have used this to compute the rates for $\not{E}_T$ events, same-sign dilepton events, $n_l=3$, 4, and 5 isolated-lepton events, and single or double $Z^0+\not{E}_T$ events from squark and gluino production at the CERN Large Hadron Collider (LHC) and the Superconducting Super Collider (SSC) for cuts inspired by the Solenoidal Detector Collaboration. We have identified and estimated several backgrounds to the various event topologies and shown that it should be possible to extract signals in several channels both at the LHC and SSC. We have shown that after accumulating one year's worth of design luminosity, it should be possible to identify a gluino with mass up to 2 TeV at the SSC, while the corresponding reach of the LHC is 1.2–1.7 TeV, depending on the luminosity.

PACS number(s): 13.85.Qk, 14.80.Ly

I. INTRODUCTION

Although the standard model (SM) has been spectacularly tested [1] in experiments at high-energy colliders, the top quark and the Higgs boson, two essential ingredients of the SM, have yet to be discovered. While the experimentally measured properties of the b quarks strongly suggest [2] the existence of an isodoublet partner (the top quark), there is no comparable evidence for the existence of a scalar particle sector that is necessary to implement electroweak symmetry breaking. The introduction of elementary scalars makes the SM (technically) unnatural since scalar-boson masses are not protected from the large radiative corrections by any symmetry of the SM Lagrangian. Within the SM framework, these corrections make the Higgs boson much heavier than the perturbative unitarity limit [3] unless the input parameters are fine tuned to uncanny precision [4]. These large corrections can, however, be compensated by introducing new degrees of freedom not included in the SM which must then manifest themselves in particle collisions at an energy $E \lesssim 1$ TeV. The exploration of physics at the TeV energy scale and the elucidation of the mechanism of electroweak symmetry breaking is the primary goal of the next generation of colliders such as the Superconducting Super Collider (SSC) in the United States and the CERN Large Hadron Collider (LHC) in Europe.

Supersymmetric particles (sparticles) are an attractive candidate for the new degrees of freedom that can ameliorate the unnaturalness of the SM. Within this framework [5], there is a spin-zero supersymmetric partner, the sfermion, $\tilde{f}_i$ for each of the chiral fermions f_i $(i=L,R)$ of the SM. Also, for each of the $SU(3)\times SU(2)\times U(1)$ gauge fields of the SM, there is a Majorana spinor field (the gaugino) with the same gauge quantum numbers as the vector bosons. Finally, the symmetry-breaking sector of any supersymmetric model consists of at least two doublets h and h' (whose vacuum expectation values (VEV's) v and v' give rise to a mass for $T_3=\frac{1}{2}$ and $T_3=-\frac{1}{2}$ fermions, respectively) together with their spin-$\frac{1}{2}$ Majorana partners, the Higgsinos $\tilde{h}$ and $\tilde{h}'$. Like the gauginos, the sfermions and the Higgsinos have the same gauge quantum numbers as their SM partners so that their interactions are fixed by supersymmetry (SUSY). The relevant effects of SUSY breaking are parametrized by the inclusion of soft supersymmetry-breaking mass terms for the scalars and the gauginos.

Unfortunately, the situation is not quite so simple because after $SU(2)\times U(1)$ breaking the particles with the same spin, color, and electric charge can mix to form the mass eigenstates. The mixing between $\tilde{f}_L$ and $\tilde{f}_R$ is proportional to the corresponding fermion mass so that, unless $\tan\beta=v/v'$ is very large, these can be considered mass eigenstates for all practical purposes (except for the scalar top system which we do not consider in this paper). If we further assume that they have a common mass at the unification scale, the masses of the squarks and sleptons at TeV energies are essentially fixed by a single parameter which we can take to be the (average) squark mass. The gluinos are the only color-octet spin-$\frac{1}{2}$ particles and so do not mix. This leaves us with the electroweak gauginos and Higgsinos which can mix once $SU(2)\times U(1)$ is broken. Their mixing patterns are generally model dependent. We work within the framework

of the minimal supersymmetric model (MSSM) which, by definition, is the extension of the SM with the minimum number of new particles and interactions. Within this framework, the gaugino-Higgsino mixing results in two charginos $\tilde{W}_-$ and $\tilde{W}_+$ and four Majorana neutralinos $\tilde{Z}_i$ ($i=1,\ldots,4$) labeled in order of increasing mass. Assuming as usual [5] that there is a common gaugino mass at the unification scale, the masses and mixing angles of the charginos and neutralinos are fixed in terms of just three parameters which we may take to be (i) the gluino mass, $m_{\tilde{g}}$ (ii) the supersymmetric Higgsino mass, $2m_1=-\mu$, and (iii) the ratio $\tan\beta$ of the VEV's of the Higgs fields of the MSSM. Together with the squark mass $m_{\tilde{q}}$ and the charged-Higgs-boson mass (which determines the Higgs sector of the MSSM [6], these parameters fix the masses and the couplings of all the SUSY particles. An assessment of the prospects for searching for SUSY at the SSC and the LHC forms the subject of this paper. We focus on the search for squarks and gluinos as these have the largest production rates at hadron colliders.

Within the framework of the MSSM, there is a multiplicatively conserved quantum number R which is $+1$ for ordinary particles and -1 for sparticles, so that sparticles can only be pair produced by collisions of ordinary particles. The cross section for the production of squark and gluino pairs is fixed by QCD in terms of $m_{\tilde{q}}$ and $m_{\tilde{g}}$. As a result of R conservation, the squarks and gluinos can only decay into lighter sparticles which then decay into even lighter sparticles until the decay cascade terminates with the production of the lightest supersymmetric particle (LSP) which is stable. A stable LSP is then unlikely to have strong or electromagnetic interactions since otherwise LSP's produced in the early Universe would have combined [7] to form exotic isotopes of atoms or nuclei which have been excluded [8] for the range of sparticle masses that can be used to stabilize the SM Higgs-boson mass. Thus, the weakly interacting LSP behaves like a neutrino in that it escapes detection in the experimental apparatus which is the reason why missing transverse energy (E_T) is generally regarded as the characteristic signature for supersymmetry. Within the MSSM, the sneutrino and the lightest neutralino $\tilde{Z}_1$ are the only possibilities for the LSP. In what follows, we will assume that the $\tilde{Z}_1$ is the LSP since the sneutrino is disfavored by the CERN e^+e^- collider LEP data combined with astrophysical considerations [9].

The cascade decay patterns [10] of squarks and gluinos have been extensively studied in the literature: it has been shown [11–14] that if the gluino or $\tilde{q}_L$ are heavy enough to decay into the charginos, these decays dominate their decay into neutralinos; for large values of $m_{\tilde{q}}$ and $m_{\tilde{g}}$, the branching fraction for the direct decays to the LSP can be 10% or smaller so that it is essential to incorporate their cascade decays in any analysis of their signals at hadron supercolliders. In contrast, $\tilde{q}_R$ (which does not couple to the charginos except via the corresponding quark Yukawa coupling which is negligible except for t squarks) can only decay into neutralinos so that for most values of SUSY parameters, it dominantly decays to the LSP [13,14] although its decays to heavier neutralinos may also be important. Finally, we note that radiative decays of the gluino which are mediated by $q\tilde{q}$ loops can also be significant [14,15], especially if the t quark is heavy as it now appears is the case [16]. The daughter charginos and heavier neutralinos produced in gluino or squark decays rapidly decay into the LSP and W, Z or Higgs bosons (which may be real or virtual) as discussed in Ref. [17]. The production of heavy quarks or gluinos at hadron supercolliders thus results in complicated events with several jets accompanied by leptons (from the leptonic decays of the W or Z bosons or the three-body decays of $\tilde{W}_i$ or $\tilde{Z}_i$) and missing transverse energy $\not{E}_T$.

In this paper, we focus on experimental signatures via which it may be possible to isolate signals for squark and gluino production at the SSC or LHC and to estimate the SM background to these signals. We have performed our computations of the signal within the framework of the MSSM which we use as a guide to masses and mixing angles. Since the decay patterns of t squarks may differ significantly [18] from those of the other squarks, we have conservatively included only five squark flavors in our calculation of the SUSY signal. The cross sections for the various events topologies are then fixed by the six parameters ($m_{\tilde{g}}, m_{\tilde{q}}, \mu, \tan\beta, m_{H^+}, m_t$) as discussed above. The signatures we study are [19]: (A) events with large $\not{E}_T$ and at least four jets, (B) events with hard, like-sign isolated dileptons+jets+$\not{E}_T$ [19,20]; (C) events with $n=3$, 4, or 5 isolated hard leptons+jets+$\not{E}_T$ [19]; (D) events with a high $p_T Z^0+\not{E}_T$+jets [19,21] possibly accompanied by an additional lepton [11]; and (E) events with two high-p_T Z^0's+jets+$\not{E}_T$ [11,12,19,22]. We have also pointed out several sources of SM backgrounds to the signals B-E which have, to our knowledge, not been considered in the literature. We have also attempted to assess the importance of these backgrounds in order to see whether or not isolated multilepton events are a viable signature for supersymmetry.

The $\not{E}_T$ signal A which is the classic signature of SUSY as well as the relevant backgrounds have been carefully studied during the 1990 Snowmass Summer Study [23,24]. These studies, which include a simple representation of the Solenoidal Detector Collaboration (SDC) and EMPACT detectors conclude that it should be possible to detect a gluino with a mass as small as 250–300 GeV via the search for $\not{E}_T$ events. It has also been shown that heavy gluinos ($m_{\tilde{g}}=1$ TeV) can be detected by hardening the $\not{E}_T$ requirement. Similar conclusions have been reached [25] for gluino detection at the LHC at the LHC Workshop held in Aachen last year. Because detailed studies already exist and because the viability of the $\not{E}_T$ signal is crucially dependent on the simulation of tails of SM backgrounds (which in turn are sensitive to the detector simulation), we will focus primarily on the multilepton event types B-E in the remainder of this paper.

Gluino pair production is a copious source of like-sign isolated dilepton pairs [19,20]. Since gluinos are Majorana particles they decay with equal likelihood into chargi-

nos with either sign so that half of the gluino pairs in which both the gluinos decay via the chargino mode contain like-sign charginos; if these charginos both decay leptonically, a like-sign dilepton+multijet+$\not{E}_T$ event results. If squarks are not much heavier than gluinos, $\tilde{q}_L\tilde{g}$ and $\tilde{q}_L\tilde{q}_L$ production can enhance the signal cross section by a significant factor [19]. The dominant SM background to like-sign dilepton production comes from the production of $t\bar{t}$ pairs where $\bar{t}\to\bar{b}l\nu$ and $t\to bq\bar{q}$ with $b\to cl\nu$. Generally speaking, the secondary lepton from the decay of the b quark is soft and often not isolated. Using a parton level simulation, it has been argued that it is possible to reduce this background to an insignificant level by imposing suitable lepton E_T and isolation requirements and by requiring at least four hard jets in the events. Since a parton level simulation of the background leads to, at most, four jets and also represents a rather simplistic simulation of the lepton isolation requirement, we have reevaluated this background using PYTHIA [26] to generate $t\bar{t}$ events. This would allow for the possibility of additional jets due to QCD radiation as well as give a better simulation of the lepton isolation. We have also estimated backgrounds to like-sign dilepton events from several other SM sources: these include

$$pp\to t\bar{t}t\bar{t}+X\ ,$$
$$pp\to t\bar{t}b\bar{b}+X\ , \tag{1}$$
$$pp\to b\bar{b}b\bar{b}+X\ ;$$
$$pp\to Wt\bar{t}+X\ ,$$
$$pp\to Wb\bar{b}+X\ ; \tag{2}$$
$$pp\to WWW+X\ , \tag{3}$$
$$pp\to W^{\pm}W^{\pm}+X\ , \tag{4}$$

where the leptons come from the decays of the heavy quarks or the W. It is worth noting that although the total cross section for the production of four tops is considerably smaller [27] than that for $t\bar{t}$ or $t\bar{t}b\bar{b}$ production, the leptons from top decays are hard and isolated so that the cuts which were instrumental in removing the $t\bar{t}$ background [20] would be rather ineffective here. Also the $t\bar{t}t\bar{t}$ events naturally have a higher-jet multiplicity and so may closely mimic the gluino signal. The same is, of course, true for $t\bar{t}W$ events.

The leptonic decays of the heavy quark and the W boson in the processes (1)–(3) also result in SM sources of isolated multilepton events. We have estimated backgrounds from these sources together with those from

$$pp\to WWZ+X\ ,$$
$$pp\to WZZ+X\ , \tag{5}$$
$$pp\to ZZZ+X\ ;$$
$$pp\to Zt\bar{t}+X\ ,$$
$$pp\to Zb\bar{b}+X\ , \tag{6}$$

as well as from the production of four vector bosons [28]. It should be noted that the bulk of multilepton events from SUSY sources do not contain a real Z boson [19] so that the processes (5) and (6) can be distinguished from the signal provided it is possible to identify leptonically decaying Z bosons at supercolliders. These processes would, of course, be a background source for the SUSY signals (D) and (E) above, for which the dominant physics background comes from the production of WZ and ZZ pairs in association with jets and from $t\bar{t}Z$ production, where one of the t's decays leptonically. In addition to these, there are other backgrounds, e.g., $t\bar{t}$ production (where the leptons from t decays accidentally reconstruct the Z) or Z production in association with jets (where the $\not{E}_T$ comes from mismeasurement of energies or from neutrinos from the decays of charm and bottom hadrons) which can fake $Z+\not{E}_T$ events while $t\bar{t}Z$ production can potentially mimic the ZZ signal if the leptons from t decays reconstruct the Z mass. A reliable estimate of these nonphysics backgrounds is difficult to obtain as the rate for such events is sensitively dependent on the details of the detector. For this reason, we will mainly focus on the like-sign dilepton and multilepton signatures, (B) and (C), in this paper and only briefly consider the prospects for detecting SUSY via high-p_T Z and $\not{E}_T$+multijet events.

The rest of this paper is organized as follows. In Sec. II we survey earlier work on SUSY signals at supercolliders and describe the improvements we have made on existing computations of the signals. We also describe our calculations of the various backgrounds discussed above. We present the results of our calculations of the signals and backgrounds in Sec. III. We also suggest two novel strategies by which it may be possible to confirm any signal in the $\not{E}_T$ or same-sign dilepton channel as being due to SUSY. We conclude in Sec. IV with a summary of our results and a brief comparison of the SSC and LHC. Formulas for the widths for the decays, $\tilde{g}\to t\bar{b}\tilde{W}_i$ and $\tilde{g}\to t\bar{t}\tilde{Z}_i$, including all terms involving m_t as well as the couplings to the Higgsino components of the chargino and neutralino, are given in the Appendix.

II. DESCRIPTION OF CALCULATIONS

As discussed in the Introduction, there is a wide variety of potentially interesting signatures via which it may be possible to search for squarks and gluinos at hadron supercolliders. As most of these analyses have been performed within the MSSM framework which we also use in this paper, we will, for brevity, confine our discussion to the refinements that we have made on existing calculations and refer the reader to the literature for details about earlier work.

In order to incorporate the experimental cuts and detector resolutions, the cross sections for the event topologies under study are usually computed using Monte Carlo techniques. Gluino and squark pairs are generated using matrix elements determined by QCD; the squarks and gluinos are then decayed into charginos and neutralinos which, in turn, further decay until the decay cascade terminates in the stable LSP. The decay patterns are model dependent; within the MSSM, they are determined by the six parameters discussed in Sec. I. We have developed a set of programs which evaluate the partial

widths of all the decay modes of the gluino, the squarks, the charginos, and all but the radiative decays, $\tilde{Z}_i \to \tilde{Z}_j + \gamma$, of the neutralinos which occur [29] via gauge or matter loops [30]. These routines, which will collectively be referred to as SUSYBF, must be interfaced with an event generator for the production of sparticles to obtain the final state which may consist of quarks, gluons, leptons, and photons or, if fragmentation and hadronization is included, of real particles. We will return to the description of our event generator shortly.

SUSYBF improves on earlier calculations of gluino decays in two respects. First, the radiative decays of the gluino [14,15] ($\tilde{g} \to g + \tilde{Z}_i$) which can be important for certain ranges of SUSY parameters have been incorporated. These two-body decays result in obviously different event topologies from the usual [10] three-body tree-level decays of the gluino. Also, for certain ranges of parameters, the radiative decay to $\tilde{Z}_4$ dominates the radiative decays; since $\tilde{Z}_4$ can decay into a real Z^0 and a lighter neutralino, the radiative decays can result in a significant contribution to the high-p_T Z^0 signal [21]. Second, we have done a new, exact calculation of the decays $\tilde{g} \to t\bar{t}\tilde{Z}_i$ and $\tilde{g} \to t\bar{b}\tilde{W}_j$. The partial widths for these decays, unlike those for light quarks, receive substantial contributions from the h-Higgsino component of the chargino or the neutralino which couples to the t-$\tilde{t}$ system via the top-quark Yukawa coupling. This is potentially important since the leptonic decays of the top quark can contribute substantially to the isolated multilepton signal. The formulas for these widths, including all terms involving m_t are given in the Appendix. We have numerically checked that our results for the branching fractions for gluino decay are in agreement with the recent paper by Bartl *et al.* [14].

In order to compute various signals from the production of squark and gluinos, we have developed a new program SUSYSM which, for any set of input values of the six MSSM parameters, generates $\tilde{g}\tilde{g}$, $\tilde{q}\tilde{g}$, and $\tilde{q}\tilde{q}$ events keeping track of squark type and flavor (this is important as the decay patterns of $\tilde{q}$ depend on the type of squark while the decays and fragmentation of the daughter quarks depend on their flavor, which is the same as that of the decaying squark) and interfaces with SUSYBF to generate various final states as given by the MSSM. The fact that SUSYSM, has the cascade decays built in is an advantage over a program like ISAJET [31] which does not discriminate between L and R squark type so that the cascades can only approximately be incorporated via decay tables generated using, e.g., SUSYBF. SUSYSM also uses the standard common block convention to keep track of event histories and a standard particle labeling scheme [32]. SUSYSM has been interfaced with the JETSET routines of Sjostrand [33] to incorporate final-state string hadronization of quarks and gluons, and also the fragmentation and decay of heavy flavors. Finally, a soft scattering event as generated by PYTHIA [26] has been superimposed to simulate the underlying event.

Our main rationale for incorporating an underlying event and hadronization into the event generator is to better simulate lepton isolation in multilepton events from supersymmetric sources. This is rather important because a parton-level generator in which final-state quarks and gluons are identified with jets, is more likely to lead to isolated leptons, and hence, to an overestimate of the multilepton signal. That a realistic simulation of lepton isolation is necessary may also be judged from the fact that in the parton-level simulation of Ref. [19], about half the trilepton events from the pair production of a 400-GeV gluino were found to have one of the leptons coming from the decay of a b or c quark; it is important to check whether or not the final-state hadronization effects lead to a different conclusion. We also mention that in a parton-level generator, the hadronic debris from fragmentation of heavy flavors is generally not correctly calculated. This contribution can affect both lepton isolation and estimates of $\not{E}_T$ in SUSY events and has been incorporated via the SUSYSM interface with JETSET.

In our simulations we are guided by the cuts used by the (SDC) [19,23]. We represent the SDC calorimeter by cells of size 0.05 in both $\Delta\eta$ and $\Delta\phi$, extending out to $|\eta| = 4.5$. We assume a hadronic energy resolution of $50\%/\sqrt{E_T}$. We further require the following.

(i) $E_T(\text{jet}) > 50$ GeV.

(ii) For isolated leptons, $p_T(\text{lepton}) > 20$ GeV, $|\eta(\text{lepton})| < 2.5$ and no hadronic activity exceeding 5 GeV in a cone with $\Delta R = \sqrt{\Delta\eta^2 + \Delta\phi^2} = 0.3$ about the lepton direction.

(iii) For the $\not{E}_T$ signal (A) we require $\not{E}_T > 150$ GeV, $\eta_{\text{jet}} \geq 4$, and transverse sphericity $S_T \geq 0.2$. We veto events with isolated leptons, to reduce backgrounds from W and heavy flavor production.

(iv) For the signals (B–E), we require $\not{E}_T > 100$ GeV.

(v) For the like-sign dilepton signal (B), we veto events with additional hard, isolated leptons—these events can contribute to the multilepton signal (C).

(vi) We have assumed that a high p_T Z^0 is always identifiable when it decays to e or μ pairs; i.e., we have assumed that the lepton daughters essentially always satisfy the criteria (ii).

The rates for the various event topologies will be discussed in the next section. Before that, we briefly describe the backgrounds to these signals as they have been discussed in the literature, and also the refinements that we have made on these existing calculations.

We begin with the cross section for like-sign dilepton + multijet + $\not{E}_T$ events which was first studied by Barnett *et al.* [20] using a parton level Monte Carlo program. They concluded that, by requiring at least four hard jets and suitable isolation and p_T cuts on the leptons, it would be possible to discover the gluino via this signature over the whole range, 180 GeV $< m_{\tilde{g}} <$ 2000 GeV. That a low-mass gluino can be seen above background at supercolliders is very significant since it is important that there should be no window of gluino masses in which the gluino can escape detection at both the Fermilab Tevatron and the SSC/LHC. This conclusion critically depends on the assumption that top-quark pair production is the only relevant background, and that it can adequately be simulated by a parton-level Monte Carlo program. The point is that in a parton-level simulation of $t\bar{t}$ events where one of the tops and one of the daughter bottoms decays leptonically (recall that this is how like-

sign dileptons events are obtained), there can be at most four quark jets in the event—three from the hadronic decay of the tops and the charm jet from one of the leptonically decaying b quarks. Then, the requirements $E_T(\text{lepton}) > 20$ GeV and $E_T(\text{jet}) > 50$ GeV are almost incompatible with the lepton isolation requirement (ii) discussed above so that the cross section is very strongly suppressed.

In view of these stringent cuts, it is imperative to check that allowing for QCD radiation (which could result in the fourth jet) does not lead to an observable background from top-quark pair production, when the lepton from b decay is isolated because the c quark is accidentally soft. Toward this end, and to better simulate the lepton isolation, we have recomputed this background using $t\bar{t}$ events as generated by PYTHIA. In addition, we have also estimated backgrounds from processes (1) and (2) discussed in Sec. I, by generating events at the parton level, and again interfacing with JETSET for heavy flavor decays and hadronization. We have estimated backgrounds from (1) by convoluting the squared matrix element for $t\bar{t}g$ production with a gluon splitting function as in Ref. [34]. We have compared our result for the total cross section with the recent paper of Barger, Stange, and Phillips [27] which uses exact QCD matrix elements and find total cross sections within a factor of 2 for all the various four heavy-quark processes, which is within the inherent theoretical uncertainty of such calculations due to variations in renormalization and factorization scales, and the particular functions used. We have renormalized our total cross section to agree with the exact results of Ref. [27]. We have performed an independent calculation of the cross section for the background from (2), including the correlations from the leptonic decay of the W. We have checked that our result reproduces the total cross section as calculated by Kunszt [35]. Finally, we have estimated the background from the electroweak production of three vector bosons and also from the production of same-sign W-boson pairs.

The processes that we have just discussed are also the leading backgrounds to the supersymmetric multilepton signals. These backgrounds have been computed essentially as described above. Finally, for reasons already discussed in Sec. I, we have not attempted to simulate the backgrounds to the Z^0 signal from either the physics processes such as (6) or the detector-dependent nonphysics backgrounds. The results of our computations of the signal and backgrounds are contained in Sec. III which we now turn to.

III. NUMERICAL RESULTS FOR SIGNALS AND BACKGROUNDS

We begin with a discussion of various supersymmetric signals obtained via the decays of gluinos and squarks using the SUSYSM program described in Sec. II. Since the incorporation of the refinements discussed in Sec. II considerably lengthens [36] the time it takes to generate a reasonable number of SUSY events, it is impractical to exhaustively scan the six-dimensional parameter space of the MSSM. In our computations of the signals, we have fixed the top-quark mass at 140 GeV, the central value obtained [37] by a fit to all available data. Assuming that $m_t > 89$ GeV [16] so that it decays into a real W boson, the main dependence of the multilepton signals on the top-quark mass comes from the variation of the gluino decay patterns with m_t. This has been studied in some detail in the literature [14,15] and will not be repeated here. We have also fixed the ratio $\tan\beta = v/v' = 2$. For a reasonable range of values of this parameter, we expect [11–15] that the $\not{E}_T$ and multilepton signals depend only weakly on this choice except for those values of $\tan\beta$ such that new decays of the gluino or the heavier chargino or neutralinos become kinematically accessible. This is elaborated upon in our discussion of Table II below. Finally, we have fixed the charged-Higgs-boson mass (which fixes the Higgs sector of the MSSM) to be 500 GeV. Our results are relatively insensitive to this value as long as $m_{H^+} \gg M_W$. We are thus left with the dependence of the signals on the parameters $m_{\tilde{g}}$, $m_{\tilde{q}}$, and μ.

The two parameters $m_{\tilde{g}}$ and $m_{\tilde{q}}$ can be used to determine the total cross sections for squark and gluino production. We show in Fig. 1(a) the total cross section for

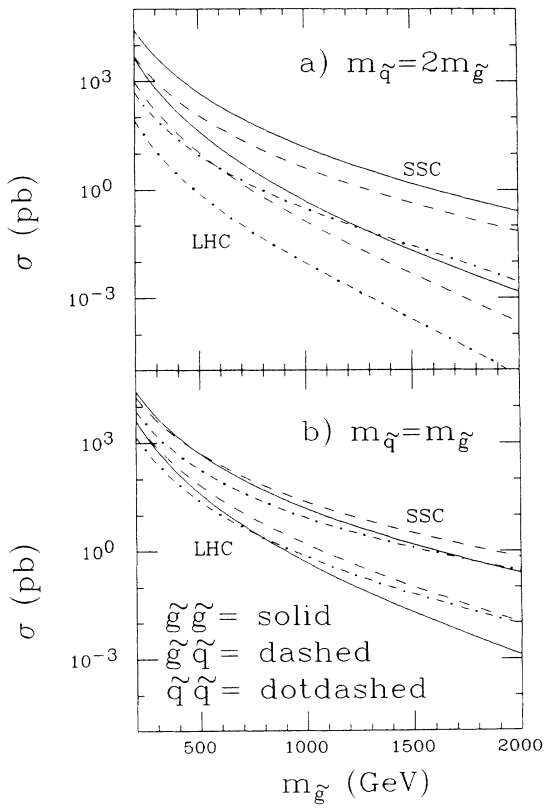

FIG. 1. Total cross sections for $\tilde{g}\tilde{g}$, $\tilde{g}\tilde{q}$, and $\tilde{q}\tilde{q}$ production at the SSC ($\sqrt{s} = 40$ TeV, upper curves) and at the LHC ($\sqrt{s} = 16$ TeV, lower curves) assuming five degenerate flavors of L- and R-type squarks, for (a) $m_{\tilde{q}} = 2m_{\tilde{g}}$, and (b) $m_{\tilde{q}} = m_{\tilde{g}}$. We have convoluted with the EHLQ set 1 parton distributions evolved in Q^2 up to $\hat{s}$.

$\tilde{g}\,\tilde{g}$ (solid, $\tilde{g}\,\tilde{q}$ (dashed), and $\tilde{q}\,\tilde{q}$ (dot-dashed) for both SSC ($\sqrt{s}=40$ TeV) and LHC ($\sqrt{s}=16$ TeV) energies, versus $m_{\tilde{g}}$, where we have fixed $m_{\tilde{q}}=2m_{\tilde{g}}$. We have assumed five flavors of degenerate squarks, and convoluted with the Eichten-Hinchliffe-Lane-Quigg (EHLQ) set 1 parton distributions [38], evolved to $Q^2=\hat{s}$. In Fig. 1(b), we show similar curves for the case of $m_{\tilde{q}}=m_{\tilde{g}}$.

The expected cross sections at the SSC for the various SUSY signals [(A)–(E)] as obtained using SUSYSM with the cuts discussed in Sec. II are shown in Fig. 2 versus (a) $m_{\tilde{g}}$, for $\mu=-150$ GeV and (b) μ, for $m_{\tilde{g}}=750$ GeV. In this figure, we have fixed $m_{\tilde{q}}=2m_{\tilde{g}}$, so that the various event topologies dominantly come from the production and subsequent decay of gluino pairs. The corresponding rates for the LHC are shown in Fig. 3 for the same values of input parameters. The curves were obtained by generating 20 000 Monte Carlo events for each set of SUSY parameters using the computer codes described in the last section. The curves labeled $\not{E}_T$ and SS correspond to cross sections for the $\not{E}_T$ signal (A) and the same-sign dilepton signal (B), respectively. The dashed curves correspond to the high-p_T Z signals (D) and (E) as labeled. The solid curves denote the cross sections for (C), the $n_{\text{lepton}}=3$ or 4 signals. Finally, we have denoted the level of the 5-lepton signals by the label 5 in those (100 GeV) bins where 5-lepton events are obtained from the 20 000 event run. It should, however, be remembered that these events are very rare so that only a few of these events are present in each bin; for instance, for the 750 GeV gluino case shown in Fig. 2(b), a cross section of 1 pb corresponds to about 235 events in our simulation. This can be seen by comparing the signal cross section to the total cross sections for gluino and squark production shown in Fig. 1(a). In those bins where there is no entry, no 5-lepton events were obtained in our simulation, although such events could possibly be picked up in a higher-statistics run.

We see from Figs. 2 and 3 that there is an observable rate for the SUSY signals (A)–(E) for a wide range of parameter values. It should, however, be noted that the cross sections at the SSC are between a factor 5–10 (for low values of $m_{\tilde{g}}$) to over a factor 100 (for very high values of $m_{\tilde{g}}$) larger than those at the LHC. It is interesting to see that for a 1-TeV gluino, the cross section for all the SUSY channels is about a factor of 25–30 larger at the SCC so that even if for an order of magnitude larger integrated luminosity at the LHC, the annual event rate for SUSY production at the SSC is about three times higher. Taking into account the higher design luminosity of the LHC, we see that SUSY events are produced at comparable rates (at least for the cuts described in Sec. II) at the two machines provided $m_{\tilde{g}}=500$ GeV. Of course, the prospects for the detection of SUSY via any of the signals under consideration depends crucially on

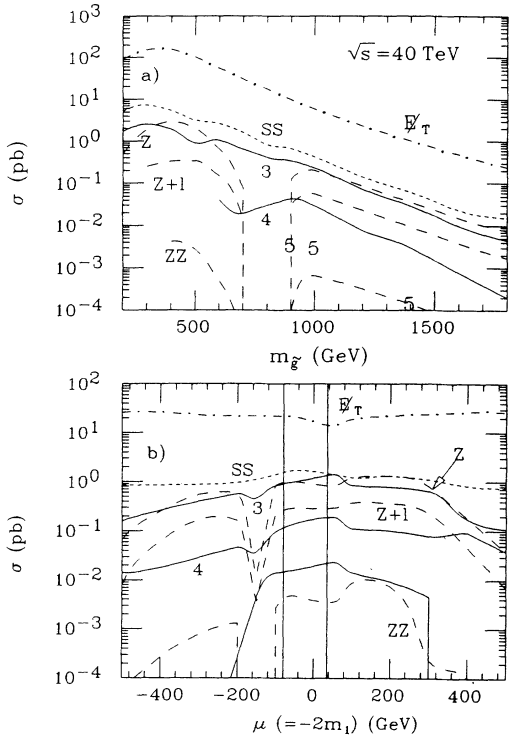

FIG. 2. Cross sections after cuts specified in Sec. II for the various event topologies discussed in the text, for $\sqrt{s}=40$ TeV. We plot (a) vs $m_{\tilde{g}}$ for $\mu=-150$ GeV, while (b) is vs μ for $m_{\tilde{g}}=750$ GeV. We take $m_{\tilde{q}}=2m_{\tilde{g}}$, $\tan\beta=2$, $m_t=140$ GeV, and $m_{H^+}=500$ GeV. The vertical bars in (b) correspond to a region excluded [19] by current LEP data.

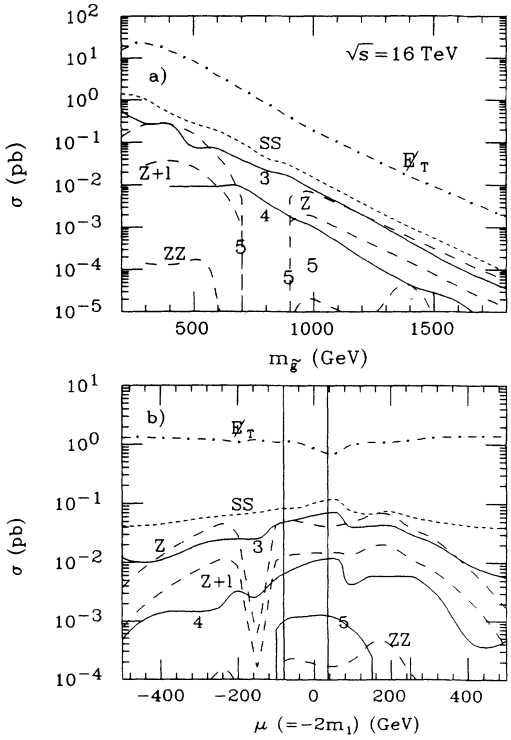

FIG. 3. Same as Fig. 2 except for $\sqrt{s}=16$ TeV, the LHC energy.

the SM backgrounds, a subject to which we shall return shortly.

At this point, it is instructive to compare the results of our calculations with the corresponding [19] computations performed using parton-level Monte Carlo programs. We have found that the cross section for $\not{E}_T$ events is only slightly altered [39] whereas the cross section for signals with isolated leptons presented here is reduced from that in Ref. [19] by a factor between 1 and 4. This is, in part, due to the more stringent isolation requirement on the lepton that we have imposed. We have also checked that, unlike as in Ref. [19], in our simulation almost all the isolated leptons come from the decay of heavy particles; i.e., leptons from decays of b and c quarks generally fail to pass the cuts.

We should emphasize that the rates for the signals shown (A–E) may be somewhat different from those shown in Figs. 2 and 3 if the squarks are lighter than $2m_{\tilde{g}}$; in this case, the contributions from $\tilde{q}\,\tilde{q}$ and, more importantly, $\tilde{g}\,\tilde{q}$ production will be considerably larger so that the event rates are enhanced. For values of $m_{\tilde{g}}$ substantially larger than M_Z, squarks cannot be much lighter than the gluino; otherwise renormalization-group evolution drives [40] $m_{\tilde{q}}^2$ to negative values before the unification scale leading to color and charge breaking minima of the scalar potential unless new Yukawa couplings are introduced into the model. In order to illustrate the contribution of $\tilde{q}\,\tilde{q}$ and $\tilde{g}\,\tilde{q}$ processes to supersymmetric signals without doing another time-consuming scan of the parameter space, we have shown the same cross sections as in Fig. 2 for $|m_{\tilde{q}}-m_{\tilde{g}}|=20$ GeV in Table I. We have illustrated our results for $m_{\tilde{g}}=300$, 600, and 1000 GeV for $\mu=-150$ GeV and -500 GeV, with other SUSY parameters fixed as before. From Fig. 1 we see that at the SSC, $\tilde{g}\,\tilde{g}$ pair production is the dominant source of 300-GeV gluinos whereas $\tilde{g}\,\tilde{q}$ production has the largest cross section for $m_{\tilde{g}}=1$ TeV; the two cross sections are about equal when $m_{\tilde{g}}=500$ GeV. We note the following.

(i) Comparing the results for the $m_{\tilde{q}}=m_{\tilde{g}}+20$ GeV case with the corresponding rates shown for the

TABLE I. Cross sections in picobarns for various event topologies from SUSY events for (a) $\mu=-150$ GeV and (b) $\mu=-500$ GeV. We take $\tan\beta=2$, $m_{H^+}=500$ GeV and $m_t=140$ GeV. Upper entries are for $\sqrt{s}=16$ TeV, while lower values are for $\sqrt{s}=40$ TeV.

$m_{\tilde{g}}$ (GeV)	$m_{\tilde{q}}$ (Gev)	$\not{E}_T$ (Gev)	SS	$3l$	$4l$	$5l$	Z	$Z+l$	ZZ
					(a)				
300	280	6	1	0.2			0.3	0.03	
		40	6	2			2	0.?	
300	320	20	3	0.7			0.3	0.02	
		150	14				2	0.09	
600	580	3	0.1	0.03			0.08	0.005	5×10^{-5}
		30	0.8	0.3			0.8	0.07	4×10^{-4}
600	620	7	0.3	0.07	0.01		0.08	0.01	2×10^{-5}
		81	5	1	0.07		0.9	0.2	6×10^{-4}
1000	980	0.2	0.01	0.01	8×10^{-4}	1×10^{-4}	0.02	3.5×10^{-3}	7×10^{-5}
		5	0.2	0.2	2×10^{-2}		0.4	6.4×10^{-2}	1.5×10^{-3}
1000	1020	0.4	0.03	0.02	2×10^{-3}	1×10^{-4}	0.02	5×10^{-3}	8×10^{-5}
		9	0.5	0.4	7.5×10^{-2}	9×10^{-3}	0.5	1×10^{-1}	1.6×10^{-3}
					(b)				
300	280	4	3	2	0.4				
		32	18	19	2				
300	320	17	4	3	0.2				
		140	28	24	2.5				
600	580	2.6	0.09	8×10^{-3}			9×10^{-4}		
		29	1.0	0.1			6.5×10^{-3}		
600	620	7	0.15	0.03	2×10^{-3}		1×10^{-3}	3×10^{-4}	
		82	2	0.3	0		1×10^{-2}	1.5×10^{-3}	
1000	980	0.2	6×10^{-3}	1×10^{-3}	1×10^{-4}		3×10^{-3}	4×10^{-4}	9×10^{-7}
		3.6	0.1	1×10^{-2}			6×10^{-2}	6×10^{-3}	4×10^{-5}
1000	1020	0.5	0.02	5×10^{-3}	6×10^{-4}	1×10^{-4}	0.01	2×10^{-3}	1×10^{-5}
		11	0.4	0.13	9×10^{-3}		0.2	5×10^{-2}	3×10^{-4}

$m_{\tilde{q}}=2m_{\tilde{g}}$ case in Figs. 2 and 3, we see that the signal rates are increased by a factor between 1 and 4, both at the SSC and LHC. Generally speaking, there is a larger increase for heavier gluinos as may be expected from changes in the production cross sections for the various subprocesses. For the same reason, the increase at the LHC is larger than at the SSC. For these values of parameters, the decay $\tilde{q}\to q\tilde{g}$ is strongly suppressed so that all squarks other than $\tilde{d}_R$ which only has small hypercharge coupling (so that its decays to a gluino can be significant) essentially decay into charginos and neutralinos; this suppresses the multiplicity of hard primary quarks and so accounts for the fact that the increase in the rate for $\not{E}_T$ events which have the requirement, $n_{\rm jet}\geq 4$, is smaller than that for the Z or multilepton events.

(ii) For $m_{\tilde{q}}=m_{\tilde{g}}-20$ GeV, the gluinos essentially decay via $\tilde{g}\to q\bar{q}\tilde{q}$ with half the squarks being left handed and half being right handed. The $\tilde{q}_R$ dominantly decay via $\tilde{q}_R\to q+\tilde{Z}_1$ whereas chargino modes form a significant fraction of $\tilde{q}_L$ decays. A high-jet multiplicity is possible only when both squarks are left handed which happens about one fourth of the time. This is the reason why the $\not{E}_T$ cross sections for the $m_{\tilde{q}}=m_{\tilde{g}}+20$ GeV case are larger than those for the $m_{\tilde{q}}=m_{\tilde{g}}-20$ GeV. This is also one reason for the same trend for the same-sign dilepton cross sections which are mainly produced by the decays of $\tilde{g}$ and $\tilde{q}_L$ pairs into same sign charginos (recall that only $\tilde{q}_L$'s couple to charginos if Yukawa couplings are negligible). In addition to this the decays of gluino into the top-quark family can also give rise to isolated, same-sign dileptons; if $m_{\tilde{g}}=m_{\tilde{q}}-20$ GeV, there is a substantial branching fraction of the decays $\tilde{g}\to tb\tilde{W}_i$ and $t\bar{t}\tilde{Z}_i$ whereas in the case $m_{\tilde{g}}=m_{\tilde{q}}+20$ GeV the gluino only decays into the first five flavors so that tops are produced only via the chargino decays of the $\tilde{b}_L$ squark.

(iii) We see that some of the cross sections are somewhat sensitive to μ. The $\not{E}_T$ cross section is more or less independent of μ, whereas those for Z production generally fall with increase in $|\mu|$. A similar trend appears to hold for the isolated lepton cross sections except when $m_{\tilde{g}}$ is rather small.

Up to now, we have fixed $\tan\beta=2$. In order to illustrate the dependence of the various signals on $\tan\beta$, we have shown the same signal cross sections for a modestly large ($\tan\beta=5$) as well as for a small ($\tan\beta=1.1$) value of $\tan\beta$ in Table II. Note that the recent discovery [41] of large radiative corrections to the mass of the Higgs bosons of the MSSM precludes us from translating the bounds [42] from the negative results for Higgs-boson searches by experiments at LEP into a limit on $\tan\beta$ when the top quark is heavy. We see that while the $\not{E}_T$ cross sections are very insensitive to the value of $\tan\beta$, those for Z production are quite sensitive to the value of this parameter. That the Z-boson cross sections increase with $\tan\beta$ is easy to understand if we remember that the Z only couples to Higgsino components of the neutralinos, and further, that for $\tan\beta=1$, only the neutralino with mass $|\mu|$ couples Z^0 to another $\tilde{Z}_i$. For the choice $m_{\tilde{g}}=600$ GeV, $\mu=-150$ GeV made in Table II(b), $|m_{\tilde{Z}_i}-150\ \text{GeV}|<M_Z$ for all the neutralinos so that decays into a real Z^0 are possible only due to small changes in the neutralino mixing patterns because $\tan\beta$ is not exactly one. In contrast, all neutralino pairs couple to Z^0 when $\tan\beta$ is sufficiently different from unity; this accounts for the large increase of the Z and $Z+l$ cross sections in Table II(a).

We now turn our attention to the prospects of seeing the various signals. This, of course entails a discussion of the various backgrounds discussed in the Introduction. Our estimates of the backgrounds to the various SUSY topologies shown in Figs. 2 and 3 are shown in Table III for the SSC and Table IV for the LHC. Also shown, for the convenience of the reader, are the signal cross sec-

TABLE II. Cross sections in picobarns for various event topologies from SUSY events for (a) $\tan\beta=5$ and (b) $\tan\beta=1.1$, with $\mu=-150$ GeV and other parameters as in Table I. Upper entries are for the LHC while lower entries are for the SSC.

$m_{\tilde{g}}$ (GeV)	$m_{\tilde{q}}$ (Gev)	$\not{E}_T$ (Gev)	SS	$3l$	$4l$	$5l$	Z	$Z+l$	ZZ
					(a)				
600	620	6	0.4	0.2	3×10^{-2}	2×10^{-3}	0.1	0.02	5×10^{-5}
		70	5	3	0.25	2×10^{-2}	1	0.2	6×10^{-4}
600	580	3	0.2	0.09	3×10^{-3}	3×10^{-3}	0.08	9×10^{-3}	6×10^{-5}
		30	1.4	0.7	8×10^{-2}		0.9	6×10^{-2}	4×10^{-4}
600	1200	3.4	0.25	0.13	0.01	9×10^{-4}	0.06	0.01	6×10^{-5}
		49	3.4	1.7	0.2		0.8	0.2	1×10^{-3}
					(b)				
600	620	6.5	0.4	0.07	2×10^{-3}		3×10^{-3}	5×10^{-4}	
		74	4	1			2×10^{-2}	4×10^{-3}	
600	580	3	0.1	5×10^{-3}			3×10^{-3}	6×10^{-4}	
		33	1	8×10^{-2}	0.03		0.04	3×10^{-3}	
600	1200	3.4	0.2	0.09	3×10^{-3}		1.5×10^{-3}	4×10^{-4}	
		49	3	1	3×10^{-2}		2×10^{-2}	7×10^{-3}	

TABLE III. SUSY cross sections in pb and various background estimates for leptonic signals at the SSC, for $m_{\tilde{g}}=300$, 1000, and 2000 GeV and $\mu=-150$ GeV, and other parameters as in Table I.

Process	σ(tot)	SS	$3l$	$4l$	$5l$	Z	$Z+l$	ZZ
$\tilde{g}\tilde{g}(300)$	6000	10	3			3	0.3	
$\tilde{g}\tilde{g}(1000)$	20	0.7	0.3	0.04	9×10^{-3}	2	0.05	8×10^{-4}
$\tilde{g}\tilde{g}(2000)$	0.25	6×10^{-3}	3×10^{-3}	5×10^{-4}		6×10^{-3}	9×10^{-4}	1.5×10^{-5}
$t\bar{t}$	1.6×10^{4}	<0.2				$387f$		
$t\bar{t}t\bar{t}$	0.5	7×10^{-3}	3×10^{-3}	2×10^{-4}		$0.05f$	$0.01f$	$3\times10^{-4}f^2$
$t\bar{t}b\bar{b}$	124	<0.003				$3f$		
$Wt\bar{t}$	2.1	0.013	2×10^{-3}			$0.1f$	$0.01f$	
$Wb\bar{b}$	341	$<9\times10^{-4}$						
$Zt\bar{t}$	12.5		<0.3	<0.04		<0.75	<0.33	$0.02f$
$W^{\pm}W^{\pm}$	1.33	0.12						
WZ	80		1				<1	
ZZ	30					<0.65		<0.11
WWW	0.4	<0.02	$<6.4\times10^{-3}$					
WWZ	0.5		<0.013	$<1.5\times10^{-3}$			<0.01	
WZZ	0.1		$<3\times10^{-3}$	$<4\times10^{-4}$	10^{-4}			$<3\times10^{-4}$
ZZZ	0.04		$<5\times10^{-4}$	$<5\times10^{-4}$	$<10^{-5}$			$<4\times10^{-4}$

tions for three values of gluino mass for $m_{\tilde{q}}=2m_{\tilde{g}}$, $\mu=-150$ GeV, with other parameters as in Figs. 2 and 3. Before turning to a discussion of the feasibility of SUSY searches a few comments about Tables III and IV are in order.

(i) The potentially biggest source of same-sign dileptons is the production of $t\bar{t}$ pairs, where the second lepton comes from the secondary decay of the bottom. We have generated 80 000 such events using PYTHIA and found no same-sign dilepton event that satisfied the cuts discussed earlier. This leads to the bound on the cross section shown in Tables III and IV. Although we have not explicitly shown this, the bounds on the multilepton backgrounds are expected to be even stronger as these are suppressed by additional factors of leptonic branching ratios.

(ii) We have computed the four top and $t\bar{t}b\bar{b}$ background as discussed in Sec. II and scaled our normalization to agree with that of the recent calculation of Ref. [27]. We have done an independent calculation of the $Wt\bar{t}$ and $Wb\bar{b}$ backgrounds, maintaining W polarization information.

(iii) Same-sign W pair production takes place by WW fusion [43] as well as by processes where quarks exchange a gluon and radiate a W pair [44]. The SM rates for same-sign dilepton production shown in Tables III and

TABLE IV. Same-sign dilepton symmetry for various values of squark and gluino masses at the LHC (top) and SSC (bottom). Cross sections are in picobarns. We have taken $\mu=-300$ GeV with other parameters as in Table I.

Process	σ(tot)	SS	$3l$	$4l$	$5l$	Z	$Z+l$	ZZ
$\tilde{g}\tilde{g}(300)$	804	1	0.3			0.25	0.03	1×10^{-4}
$\tilde{g}\tilde{g}(1000)$	0.65	0.015	8×10^{-3}	1×10^{-3}	1×10^{-4}	7×10^{-3}	2×10^{-3}	2×10^{-5}
$\tilde{g}\tilde{g}(2000)$	1.7×10^{-3}	2.7×10^{-5}	1.2×10^{-5}	5×10^{-7}	9×10^{-8}	2×10^{-5}	5×10^{-6}	1×10^{-7}
$t\bar{t}$	3.2×10^{3}	<0.04				$79f$		
$t\bar{t}t\bar{t}$	0.03	5×10^{-4}	2×10^{-4}	1×10^{-5}		3×10^{-3}	$6\times10^{-4}f$	$2\times10^{-5}f^2$
$t\bar{t}b\bar{b}$	17	1×10^{-4}	$<1\times10^{-4}$			$0.4f$		
$Wt\bar{t}$	0.65	3.4×10^{-3}	7.3×10^{-4}			$0.03f$	$3\times10^{-3}f$	
$Wb\bar{b}$	181	$<5\times10^{-4}$						
$Zt\bar{t}$	1.75		<0.05	$<4\times10^{-3}$		<0.07	<0.05	
$W^{\pm}W^{\pm}$		0.034						
WZ	30						<0.4	
ZZ	10					<0.22		<0.04
WWW	0.18	$<9\times10^{-3}$	$<2\times10^{-3}$					
WWZ	0.15		$<4\times10^{-3}$	$<5\times10^{-4}$			$<4\times10^{-4}$	
WZZ	0.037		$<1\times10^{-3}$	$<1\times10^{-4}$	$<3\times10^{-5}$			$<1\times10^{-4}$
ZZZ	0.016		$<2\times10^{-4}$	$<2\times10^{-4}$	$<3\times10^{-6}$			$<2\times10^{-4}$

IV have been obtained [45] from the computation of the l^+l^+ rate from W^+W^+ production for the same cuts ($|\eta_l| < 2.5$, $pT_l > 20$ GeV) on the leptons as in the case of the signal. No isolation of $\not{E}_T$ requirement has been imposed so that the background rate shown is an overestimate. We have added in the l^-l^- rate to this assuming that $\sigma(W^+W^+)/\sigma(W^-W^-)=1.5$ for both the gluon-exchange process (for which this has been explicitly computed by Dicus and Vega [44]) and the W^-W^- fusion process (which probably overestimates this background). In the computation, the Higgs boson mass has been set to 1 TeV. The results are insensitive to this choice since the production of transversely polarized W pairs (which form the bulk of the cross section) is insensitive to m_H.

(iv) The total cross section for $Zt\bar{t}$ production has been estimated from both gg and $q\bar{q}$ initial states. For the latter, we have retained only those diagrams where the Z is radiated off the incoming quarks since the contribution of the diagrams where the Z is radiated off the final-quark lines is suppressed because the gluon propagator is $\sim 1/m^2(Zt\bar{t})$ as opposed to $\sim 1/m^2(t\bar{t})$ in the case of initial-state radiation.

(v) Backgrounds to multilepton events from the production of three vector bosons have been estimated by multiplying the corresponding production cross sections calculated by Barger and Han [46] by appropriate branching fractions. Thus the entries in Tables III and IV are, once again, upper limits on these backgrounds.

(vi) We have also computed the upper limits on the multilepton production from four vector boson sources using the total cross sections from Ref. [28]. We find that these result in ~ 10 same-sign dilepton and trilepton events per year at the SSC and have much smaller rates for $n_l > 3$. For this reason, we have not listed these cross sections in the Tables.

We now turn to the prospects for seeing SUSY via the different event topologies for which the cross sections are shown in Figs. 2 and 3.

$\not{E}_T$ signature

The production of $\not{E}_T$ events is the most carefully studied signature of SUSY at hadron colliders. Detailed simulations [23–25] of the SM background have been done and it has been concluded that it should be possible to discover the gluino with a mass up to about a TeV both at the SSC and the LHC, assuming an integrated luminosity of 10^4 pb^{-1}. The complexity of the simulations make it difficult to quote a precise discovery limit at either the SSC or the LHC. It has further been shown that despite the softer $\not{E}_T$ spectrum, it should also be possible to detect a gluino if $m_{\tilde{g}}=300$ GeV. In view of these conclusive studies, we have made no attempt to reexamine the viability of this signal: the cross sections shown in Figs. 2 and 3 are presented only to give the reader an idea of the number of events of this type that may be expected, and how these compare with the other signals considered in this paper.

We note here that SUSY $\not{E}_T$ events may be differentiated from SM $\not{E}_T$ events with multiple jets in that SUSY events will likely contain a larger fraction of high-p_T B mesons. This is due to two reasons: (1) heavy gluinos, charginos, and neutralinos decay to heavy flavors with a large rate while standard-model heavy flavor production is suppressed relative to light flavor production, and (2) the charginos and neutralinos frequently decay to the lightest Higgs scalar, which in turn decays almost always in the MSSM to $b\bar{b}$. Multiple B production from QCD occurs at a large rate [27,47], however, it should be noted that most of these would be in the beam direction, and such events would not typically have large $\not{E}_T$; in contrast, B mesons from SUSY sources are dominantly central. Whether the displaced vertices from B decays can be detected is an experimental issue. While such tagging is probably impossible along the direction of the beams (due to large numbers of tracks), it is conceivable in the central region. The percentage of events with n identified B's is shown in Fig. 4 for squark and gluino production at the SSC for $m_{\tilde{g}}=300$ and 1000 GeV. We have fixed $m_{\tilde{q}}=2m_{\tilde{g}}$, $\mu=-150$ GeV and the other parameters as in Figs. 2 and 3. We have also assumed a detection efficiency of 50% for each displaced B vertex identification. We see that even for the lower gluino mass case, 0.2% of gluino events which pass the cuts of Fig. 2 have $n_b \geq 4$ (corresponding to 3000 events/SSC year) whereas about 150 events with $n_b \geq 7$ may be expected if $m_{\tilde{g}}=1000$ GeV. The point here is that a given sample of $\not{E}_T$ events from SUSY should be unusually rich in the number of B's present, relative to a similar sample from SM background sources. This could lend confidence to any claim of the existence of a SUSY $\not{E}_T$ signal. We should stress, however, that the expected multiplicity of B's may be quite different from that shown in the figure if the efficiency for B identification differs substantially from 50%.

Same-sign dilepton signature

As discussed above, top-quark pair production is potentially the main source of same-sign dilepton pairs at the SSC. Since the second lepton is produced by the decay of a secondary b quark, isolation and p_T cuts discussed in the last section are very effective [20] in eliminating this source of dileptons in the SM. We have confirmed this result. In our simulation of 80-K top-quark events at each collider, we find that no events pass the cuts giving us an upper bound of 0.2 pb (0.04) on the background, to be compared with a signal cross section of 0.07 pb (0.015 pb) (for $m_{\tilde{g}}=1$ TeV) at the SSC (LHC). Of course, the same-sign dilepton production rate from $t\bar{t}$ production may well be considerably smaller than the bound in the table. To examine whether the background is indeed smaller than the signal cross section for 2-TeV gluinos at the SSC, would require an increase of a factor of $\sim 10^3$ in computer time. Fortunately, however, this is not necessary, since it is possible to drastically enhance the signal-to-background ratio for very heavy gluinos by imposing harder cuts on p_T(jet) and the total scalar energy in the event as we will see below.

Turning to the other sources of SS dileptons listed in Tables III and IV, we see that even after the cuts, there

are small but observable cross sections from $t\bar{t}t\bar{t}$ production, from W production in association with top-quark pairs, from the production of three W bosons and from the production of same-sign W pairs. The background contributions from $t\bar{t}b\bar{b}$ and $Wb\bar{b}$ are negligible after the cuts; in our simulation of 40–80-K events of each type, we found no events from these sources at the SSC and just two same-sign dilepton events from $t\bar{t}b\bar{b}$ production at the LHC. We thus conclude that at the SSC (LHC), we expect a same-sign dilepton cross section from SM sources after cuts to select out SUSY events to be smaller than about 0.15 pb (0.03 pb) which is considerably smaller than the signal for $m_{\tilde{g}}=1$ TeV even for the heavy-squark case at least at the SSC. It should be noted that the bulk of the background comes from same-sign W events, which should have very different event topology from the signal, especially for large values of $m_{\tilde{g}}$—in particular, aside from the two jets with $p_T \sim M_W$, we do not expect a high-jet multiplicity in these events. Assuming that this will make it possible to separate the signal from the leading contribution to the same-sign W background, we see that the remaining SM cross sections are considerably smaller than the signal from a 1-TeV gluino both at the SSC and the LHC.

To see whether it is possible to probe gluino masses in excess of 1 TeV, we have studied the scalar E_T, invariant mass of the event and E_T(jet) distributions (for the three hardest jets). We find that the scalar E_T distribution, shown by the solid curve in Fig. 5, is the best discriminator of the SUSY signal against SM backgrounds from $Wt\bar{t}$ production (dashed) or $t\bar{t}t\bar{t}$ production (dot-dashed). We expect that this distribution is even softer for same-sign dilepton events from $t\bar{t}$ production. By making a cut on the total scalar transverse energy $\sum E_T > 1400$ GeV, we expect about 190 same-sign dilepton events per 10^4 pb^{-1} at the SSC even for $m_{\tilde{g}}=\frac{1}{2}m_{\tilde{q}}=1.6$ TeV with essentially no background. Over half these events contain a jet with $E_T > 600$ GeV with the two other jets having E_T in excess of about 200 GeV, while n_{jet} is typically ≥ 4. We have checked that at the SSC we expect 50 same-sign dilepton events per year for $m_{\tilde{g}}=0.5m_{\tilde{q}}=2$ TeV after the $\sum E_T > 1400$ GeV cut. This rate falls to 11 (1.7) events for $m_{\tilde{g}}=0.5m_{\tilde{q}}=2.5$ TeV (3 TeV). It thus appears that the SSC should be able to probe a gluino mass in excess of 2 TeV with about a year of running even allowing for a factor 2 uncertainty in our calculations. For the same integrated luminosity, the LHC becomes rate limited once the gluino mass exceeds about 1200 GeV while for an order of magnitude larger luminosity, the reach may be increased by about 500 GeV.

Up to this point, our discussion of same-sign dileptons has focused on the case $m_{\tilde{q}}=2m_{\tilde{g}}$. As we have seen in Table I somewhat different rates are expected if the gluinos and squarks are approximately degenerate. Furthermore, if $\tilde{g}\tilde{q}$ production is significant, we expect considerably more positive dilepton pairs than negative ones since the proton has twice as many u-type valence quarks as it has d-type valence quarks. This is illustrated in Table V where we have separately shown the cross sections for positive and negative dilepton pairs for $m_{\tilde{g}}$ slightly bigger than $m_{\tilde{q}}$. We have also shown the dilepton symmetry A defined by

$$A=\frac{\sigma(++)-\sigma(--)}{\sigma(++)+\sigma(--)} . \tag{7}$$

We should note that for $m_{\tilde{g}}=250$ GeV, about 13 SS dilepton pairs of each sign were obtained in our simulation, so that the results shown may have considerable statistical fluctuations, whereas for the $m_{\tilde{g}}=750$ GeV case

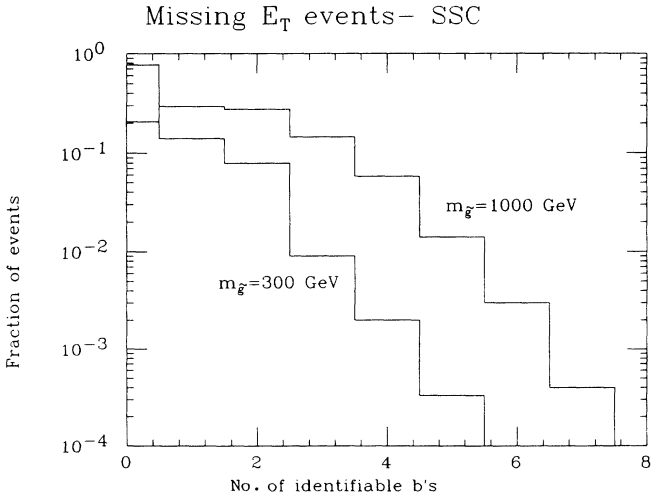

FIG. 4. Histograms of percentage of $\not{E}_T$ events from SUSY at the SSC containing n identifiable B mesons. We have assumed 50% detection efficiency for resolving a displaced B decay vertex. Parameters are as in Fig. 2, except we plot for $m_{\tilde{g}}=300$ and 1000 GeV.

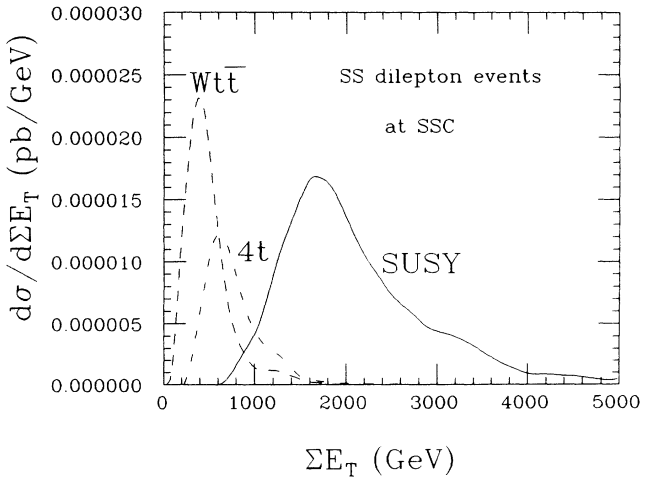

FIG. 5. Distribution in total scalar transverse energy ($\sum E_T$) in SUSY same-sign dilepton events at the SSC for $m_{\tilde{g}}=1600$ GeV, and other parameters as in Fig. 2. We also show the corresponding background contributions from $Wt\bar{t}$ and $t\bar{t}t\bar{t}$ events for $m_t=140$ GeV.

TABLE V. Same-sign dilepton asymmetry for various values of squark and gluino masses at the LHC (top) and SSC (bottom). Cross sections are in picobarns. We have taken $\mu=-300$ GeV with other parameters as in Table I.

$m_{\tilde{g}}$	$m_{\tilde{q}}$	$\sigma(++)$ (pb)	$\sigma(--)$ (pb)	A
260	250	1.7	0.4	0.6
		9.2	7.8	0.08
510	500	0.15	0.07	0.3
		0.9	0.6	0.2
760	740	0.03	0.012	0.4
		0.3	0.2	0.2
1020	1000	4.5×10^{-3}	1.8×10^{-3}	0.4
		0.08	0.04	0.33

54 (68) l^+l^+ and 36 (28) l^-l^- events were obtained at the SSC (LHC). We observe that for smaller values of $m_{\tilde{g}}$, the asymmetry tends to be larger at the LHC than at the SSC. This is because at the LHC energy the $\tilde{g}\,\tilde{q}$ and $\tilde{g}\,\tilde{g}$ cross sections are already equal for $m_{\tilde{q}}=m_{\tilde{g}}=200$ GeV. Notice that we have shown Table V for the case $m_{\tilde{q}}<m_{\tilde{g}}$ for which the same-sign dilepton rate is considerably smaller (see Table I) than that for the other case. We have checked though that when $m_{\tilde{g}}$ is slightly smaller than $m_{\tilde{q}}$, the asymmetry is considerably reduced, e.g., even for the 1-TeV case, we find an asymmetry of about 0.1. We note that since A is obtained as a difference of large cross sections, the values shown in the table should only be regarded as indicative.

Multilepton signals

We see from Figs. 2 and 3 that there are observable rates for $n_l=3$, 4, and 5 lepton signals for some range of gluino masses. As seen from Tables I and II, these rates do depend somewhat on the model parameters—in particular, they tend to be smaller if $|\mu|$ is large. Nevertheless, there are wide ranges of parameter values where $\gtrsim 1000$ trilepton events and $\gtrsim 100$ 4-lepton events are expected per SSC year. The cross sections at the LHC are 1–2 orders of magnitude smaller depending on the value of $m_{\tilde{g}}$, so that if the anticipated high luminosity can indeed be achieved at the LHC, a comparable event rate should be possible except at the highest values of the gluino mass. We see from Table III that the rates for trilepton and 4-lepton events from $Zt\bar{t}$ production at the SSC can be potentially as large as the SUSY signal for $m_{\tilde{g}}=1$ TeV, $\mu=-150$ GeV, and $\tan\beta=2$. It should, of course, be recognized that the background shown corresponds to the total cross section before any cuts. The production of three vector bosons at the SCC leads to a total cross section for trilepton (4-lepton) production of 0.02 pb (0.003 pb). It is instructive to note that the background events either contain a leptonically decaying Z boson, or have very little hadronic activity (WWW backgrounds to trileptons). In contrast, by comparing the 3- and 4-lepton cross sections in Fig. 2 with the corresponding $Z+l$ and ZZ production rates, we see that only a small fraction of SUSY events contain a real Z boson. By vetoing events with an identified Z boson, and (for heavy gluinos) by requiring a large amount of hadronic activity (as in Fig. 5), it should be possible to separate the SUSY signal from the SM background. In addition, up to 100 5-lepton events may be expected annually at the SSC. SM backgrounds to these appear to be negligible. We conclude that at the SSC, it should be possible to detect the gluino with a mass up to 1000–1400 GeV using the multilepton channel, the precise reach being dependent on other model parameters.

The situation at the LHC is roughly similar. Here, the $Zt\bar{t}$ background rate may be more than five times the trilepton signal for $m_{\tilde{g}}=1$ TeV, whereas multiple vector-boson production contributes at about the same rate as the signal. Note also that the fraction of Z events in the signal is somewhat larger than at the SSC. Once again, by vetoing events with a real Z boson and by requiring sufficiently large hadronic activity, it should be possible to reduce the backgrounds from these sources. Thus while the identification of a 1-TeV gluino may well be possible in the multilepton channel (identification of leptonically decaying Z bosons will probably be crucial though), the small cross sections suggest that the high-luminosity option will be necessary in order to search for a 1-TeV gluino via its multilepton signature.

Although we have seen that the physics backgrounds to the multilepton events from squark and gluino sources can be reduced to acceptable levels by a judicious choice of cuts, it is worth pointing out that unusual event topologies can also result if the rate for either (i) hard collisions of two pairs of partons [48] in the same proton, or (ii) overlay of events from two independent scattering events within the time resolution of the detector is important. The rate for the former depends on the size of the proton which we have taken to be 15 mb (corresponding to a radius of 0.7 fm [49]. The chance for two superposed events obviously depends on the luminosity and the time resolution Δt of the detector. In our estimates, we have taken $\Delta t=100$ ns [50]. If better resolution is achieved,

the backgrounds will be proportionally smaller. Assuming an integrated luminosity of $10^{33}/\text{cm}^2\,\text{s}$, we find that at the SSC (LHC) the total cross sections from these sources are

$$\sigma(W^+W^+)=5\text{ pb }(1.3\text{ pb}),$$
$$\sigma(Wt\bar{t})=1\text{ pb }(0.1\text{ pb}), \tag{8}$$
$$\sigma(t\bar{t}t\bar{t})=0.034\text{ pb }(1.4\times10^{-3}\text{ pb}),$$

to be compared with the total rates in Tables III and IV. We see that the W^+W^+ rate is considerably larger than the rate expected from W^+W^+ production in single-parton collisions. It should be noted, however, that the W boson is dominantly produced along the beam pipe in double-parton collisions so that the lepton p_T should exhibit the usual Jacobian peak at $M_W/2$. Furthermore, these events will have limited jet activity so that we do not anticipate this background to be a problem. It should be stressed, however, that double-parton scattering is a large source of isolated same-sign leptons at supercolliders so that caution must be exercised in the analysis of the data. We see from Eq. (8) that the cross section from $Wt\bar{t}$ production is about half the QCD value at the SSC though it is small at the LHC. Once again, it should be possible to reduce this to negligible levels by a cut on the lepton p_T with only a small loss of signal. The contribution of multiple scattering to $t\bar{t}t\bar{t}$ production is small. Before closing this discussion, we note that these backgrounds may be more significant if the LHC is indeed operated at a luminosity of $50\times10^{33}/\text{cm}^2\,\text{s}$. In this case, the contribution from event overlay [which makes up more than half the rate in Eq. (3.2)] would increase by a factor 50 unless the timing could be significantly improved from the 100-ns figure assumed in our calculation.

High-p_T $Z+E_T$ events

The cascade decays of squarks and gluinos can lead to the production of high-p_T Z bosons in association with jets together with $\not{E}_T$. The rate for Z production is sensitive to the model parameters and may be very small if $\tan\beta$ is close to unity. There are, nevertheless, substantial ranges of SUSY parameters where the cross section for high-p_T Z production, with the Z decaying into an e or μ pair, leads to 10^3-10^4 (10^2-10^3) events per 10^4 pb^{-1} of integrated luminosity at the SSC (LHC). We also see that there are about one-tenth as many events which contain an additional hard, isolated lepton whereas as many as $\sim$10–100 gold-plated events [22] with several jets together with two cleanly identified leptonically decaying Z bosons may be expected annually at the SSC or the high-luminosity version of the LHC.

The dominant physics background to high-p_T Z plus $\not{E}_T$ events comes from Z production in association with another W or Z or a t quark pair. The leptonic decay of the associated vector boson or t quark can then lead to $\not{E}_T$. It may be possible to substantially reduce the background from WZ and ZZ events by requiring substantial additional jet activity in the event. The more important background is from $Zt\bar{t}$ production where one of the top quarks decays hadronically and the other leptonically. The leptonic decay of the top quark is essential in order for there to be a substantial amount of $\not{E}_T$ (this is necessary to eliminate the background from high-p_T Z production which has an enormous cross section). The entries in Tables III and IV correspond to upper limits which have been obtained by multiplying the total cross section by appropriate branching fractions. We stress that actual backgrounds will be somewhat smaller once the $\not{E}_T>100$-GeV cut is imposed on the events. It is nevertheless worth stressing that these events which have similar topology as the signal; i.e., several jets (from the decay of the top quarks) together with $Z+\not{E}_T(+l)$ have a background rate similar in magnitude to the signal. Although it may be possible to further enhance the signal relative to background by making cuts on, for example, $\sum E_T$, it should be kept in mind that the smallness of the cross sections may preclude the possibility of strong cuts which substantially reduce the signal. We have made no attempt to see whether this is possible because of other detector-dependent backgrounds discussed below.

In our analysis of Z events, we have assumed that Z bosons decaying via e or μ pairs can always be identified; i.e., we have assumed that any e^+e^- or $\mu^+\mu^-$ pair that reconstructs to the Z mass (within experimental resolution) will be identified as a Z boson. There are, however, other sources of e and μ pairs which can accidentally reconstruct to the Z mass and, therefore, be indistinguishable from a Z event. The biggest source of these "fake Z" events is $t\bar{t}$ production where both top quarks decay into a lepton with the same flavor and the leptons accidentally reconstruct the Z. The factor f that represents the fraction of lepton pairs that reconstruct the Z boson is both process and detector dependent. Because of the enormous cross section for $t\bar{t}$ production, we see from Tables III and IV that if f is substantially larger than few parts in a thousand, the $t\bar{t}$ background becomes comparable to the SUSY signal, both at the SSC and the LHC. Furthermore, these events all have a substantial amount of $\not{E}_T$ from the two neutrinos. For heavy gluinos, it may be possible to distinguish these events from the SUSY signal (from the differences in accompanying jet activity) but for smaller values of $m_{\tilde{g}}$ this may be very difficult. We have also listed other sources of "fake Z" events in Tables III and IV together with our rate estimates in terms of f. (It should be clear that the fraction is process dependent although we use the same symbol for convenience of notation.) We see that a detailed simulation of several "fake Z" processes (including the effects of finite detector resolution) is necessary in order to assess the viability of the various Z signals.

SUSY Higgs-boson production by $t\bar{t}$ fusion, for instance, $gg\to t\bar{t}H$ can be yet another source of multilepton as well as $Z+\not{E}_T$ events if the Higgs boson is heavy and decays into vector bosons or t quarks, and several of the final-state particles decay leptonically. The cross section for this has been estimated within the framework of the MSSM by Dicus and Willenbrock [51]. Of course, only the heavier Higgs scalar (H) and the pseudoscalar (A) can decay into t pairs or vector bosons, while the light Higgs boson (h) still decays to $b\bar{b}$. For $m_{H^+}=500$ GeV and

$m_t = 100$ GeV, these authors estimate the cross sections to be $\sim 10^{-2}$–10^{-1} pb at the SSC depending on the value of $\tan\beta$. Folding in the leptonic branching fractions, we see that these processes do not significantly contribute to the SUSY signal. Two points are worth noting here: (i) the rate for Higgs-boson production from bottom-quark fusion ($gg \to b\bar{b}H$) can be much larger than the corresponding top-quark rates, but the lepton isolation requirement should eliminate these events, and (ii) the cross section increases by about a factor 5 if the charged-Higgs-boson mass is 200 GeV so that even if M_{H^+} is just large enough for vector-boson decays to be accessible, it is unlikely that this process will hamper the detection of SUSY signals from squarks and gluinos (particularly if it is possible to veto leptonically decaying Z bosons). We should note that within the SM the cross section for $t\bar{t}H$ production is somewhat larger than the SUSY case since there is no $\tan\beta$ factor in the top-quark Higgs-Yukawa coupling. Finally, we observe that at the SSC, the cross section for the related process $gg \to t\bar{t}H^{\pm}W^{\mp}$ is [52] smaller than $\sim 10^{-2}$ pb for $m_{H^+} = 500$ GeV so the multilepton rates from this are negligible.

IV. SUMMARY AND CONCLUDING REMARKS

The resolution of the gauge hierarchy problem strongly indicates that new physics beyond the SM must manifest itself in collisions of elementary particles at TeV energies. Although supersymmetry provides [53] an elegant way to stabilize the gauge hierarchy, it is not the only viable extension of the SM. However, a recent analysis [54] of the renormalization-group evolution of the electroweak and strong-interaction couplings measured at LEP shows that, unlike the SM, the MSSM allows for a unification of the strong and electroweak interaction at an energy scale compatible with the measured lower limits on the proton lifetime, if the effective SUSY-breaking scale is $\lesssim 1$ TeV. The same analysis excludes SUSY models with additional pairs of Higgs doublets but, of course, extra singlet superfields are allowed since, to lowest order, these do not affect the evolution of gauge couplings. This may be regarded as further motivation for weak scale supersymmetry, and of the MSSM as the effective theory at low energy.

In this paper, we have computed the rates for various promising-event topologies from the production and subsequent decays of squarks and gluinos at the LHC and the SSC using the MSSM as a guide to sparticle masses and mixing angles. These event topologies, which are listed in Sec. I, include $\not{E}_T$ events, same-sign dilepton events, events with $n_l = 3$, 4, and 5 hard, isolated leptons and, finally, events containing one or two high-p_T Z bosons, possibly in association with an additional isolated lepton. We have also listed various SM sources that lead to the same event topologies and attempted to estimate the rates from these sources in order to assess whether it is possible to detect the SUSY signal above the background.

To compute the supersymmetric signal rates, we have constructed a new Monte Carlo generator, SUSYSM which, for any set of MSSM input parameters, generates $\tilde{g}\tilde{g}$, $\tilde{g}\tilde{q}$, and $\tilde{q}\tilde{q}$ events and then decays them via the various cascades as given by the minimal model. Hadronization has been incorporated by interfacing SUSYSM with the JETSET routines and the underlying event has been simulated by overlaying a soft-scattering event generated using PYTHIA. We use SUSYSM, incorporating SDC-inspired cuts described in Sec. II, to compute rates for the various signals. Our computation of the various backgrounds is also discussed there.

The main results of this paper are the signal cross sections for the various event topologies shown in Figs. 2 (SSC) and 3 (LHC) for $m_{\tilde{q}} = 2m_{\tilde{g}}$ and $\tan\beta = 2$ and in Tables I and II for other parameter choices. Our estimates of SM backgrounds to the SUSY signal are shown in Tables III (SSC) and IV (LHC). Since detailed studies of the $\not{E}_T$ background to SUSY already exist in the literature, we present signal rates for this category of events only for comparison with leptonic signals, and remark that SUSY sources of $\not{E}_T$ events should be unusually rich in content of B mesons as compared to SM $\not{E}_T$ events. These B's may be tagged by displaced decay vertices using a microvertex detector.

We have mainly focused our attention on the same-sign dilepton and isolated multilepton events from supersymmetry. The SM contributions to these event topologies are shown in Tables III and IV. After cuts designed to separate the SUSY signal from the background, the biggest source of same-sign dileptons is most likely to be same-sign W production. We have argued that for the range of squark and gluino masses where the background is significant, the SUSY events can be distinguished because they have very large hadronic activity (see Fig. 5) as well as jet multiplicity. This leaves us with small but observable backgrounds from $Wt\bar{t}$ and $t\bar{t}t\bar{t}$ events. These backgrounds can be reduced to an insignificant level by a cut on $\sum E_T$ in the event. We have concluded that even allowing for a factor 2 uncertainty in the calculation of the cross section, it should be possible to probe $m_{\tilde{g}}$ in excess of 2 TeV with a year's running at the SSC and about 1.2 TeV (1.7 TeV) at the LHC with a luminosity of $10^{33}/\text{cm}^2\,\text{s}$ ($10^{34}/\text{cm}^2\,\text{s}$). If same-sign dileptons are coming mainly from gluino pair production, then the event sample should be equally divided between $++$ and $--$ dileptons. However, if the squark is somewhat lighter than the gluino, then an asymmetry may exist, and there should be more $++$ than $--$ events produced, which can help yield information about the SUSY source of the dileptons.

We have also seen that for a wide range of sparticle masses there are observable signals at the SSC in the multilepton channels even if $m_{\tilde{g}}$ exceeds 1 TeV. At the LHC, it will be difficult to probe considerably larger masses in these channels unless the machine is operated at the higher luminosity, in which case there may be additional backgrounds from multiple collisions during each bunch crossing. It should, however, be stressed that the signal is essentially rate limited (after cuts) so that the reach of these colliders will be somewhat larger if they are operated for several years. We have also computed the rates for

high-p_T $Z+\not{E}_T$ events as shown in Figs. 2 and 3 as well as in Table I–IV. We see that although these rates are rather sensitive to model parameters, a substantial number of these characteristic events may be expected for a large part of the parameter space. Aside from real Z backgrounds, we have seen that there are other detector-dependent backgrounds where dileptons of the same flavor accidentally reconstruct the Z mass (see Table III). The rates for these "fake Z" events which we have shown can be potentially large, are sensitive to details of the detector so that simulations beyond the scope of the present analysis are necessary to assess the viability of this signal.

To conclude, we have studied the rates for the production of $\not{E}_T$ events, same-sign dilepton and isolated multilepton events, and high-p_T $Z+\not{E}_T$ events from the production and subsequent decay of squarks and gluinos at the SSC and LHC. In our computation, we have incorporated all the cascade decays as given by the MSSM, and evaluated signals using SDC inspired detector parameters and cuts. We have also identified and estimated several new backgrounds to the above signals and have shown that it should be possible to identify the signal above background in several channels, both at the SSC and the LHC. In the same-sign dilepton channel it should be possible to probe a gluino mass exceeding 2 TeV at the SSC and 1.2–1.7 TeV at the LHC (depending on luminosity) after just one year of running. Cascade decays of squarks and gluinos provide a rich variety of promising channels in which to search for SUSY signals at hadron supercolliders; discovery of a signal in any one channel ought to be verified by the simultaneous presence of signals in other channels at roughly the expected rates before a signal for sypersymmetry can be claimed.

ACKNOWLEDGMENTS

We thank V. Barger, A. Bartl, K. Hikasa, G. Kane, W. Majerotto, B. Mosslacher, J. Ohnemus, A. Stange, and R. Vega for helpful discussions, and M. Bisset and M. Drees for comments on the manuscript. This work was supported in part by the U. S. Department of Energy, Grants No. DE-AM03-76SF00235 and No. W-7405-ENG-82, Office of Energy Research (KA-01-01), Division of High Energy and Nuclear Physics. This work was supported in part by the U. S. Department of Energy.

APPENDIX

We present formulas for the partial widths for the decays $\tilde{g}\to t\bar{b}\tilde{W}_i$ and $\tilde{g}\to t\bar{t}\tilde{Z}_j$ including the coupling of the h-Higgsino components of the charginos and neutralinos via top-quark family Yukawa interactions. In the notation of Refs. [11] and [15], the chargino couplings are given by

$$\mathcal{L}=iA^d_{\tilde{W}_i}\tilde{u}^\dagger_L\bar{\tilde{W}}_i\frac{1-\gamma_5}{2}d+B_{\tilde{W}_i}\tilde{u}^\dagger_R\bar{\tilde{W}}_i\frac{1-\gamma_5}{2}d$$
$$+\tilde{d}^\dagger_L\bar{\tilde{W}}^c_i\left[iA^u_{\tilde{W}_i}\frac{1-\gamma_5}{2}+B_{\tilde{W}_i}\frac{1+\gamma_5}{2}\right]u+\text{H.c.}\ , \tag{A1}$$

where

$$B_{\tilde{W}_-}=-f_u(-1)^{\theta_-}\cos\gamma_R\ , \tag{A2a}$$

and

$$B_{\tilde{W}_+}=f_u(-1)^{\theta_+}\theta_y\sin\gamma_R\ . \tag{A2b}$$

Here, f_u, the up-quark Yukawa coupling, is as given in Ref. [15]. $A^d_{\tilde{W}_i}$, $A^u_{\tilde{W}_i}$, γ_L, and γ_R are obtained by diagonalization of the chargino mass matrix and can be read off from Ref. [11]. The mass matrix used in our calculation differs from that in Ref. [11] in that the signs of all the off-diagonal terms are reversed, so that Eqs. (2.6), (2.7), and (2.9) of Ref. [11] require appropriate modification. The coupling of the neutralinos to the $t\bar{t}$ system are given in Ref. [15]. Once again, the eigenvector components $v_i^{(j)}$ may be obtained from the neutralino mass matrix in Ref. [11] but with the signs of the vacuum expectation values reversed.

Neglecting the b-quark Yukawa coupling the decay $\tilde{g}\to t\bar{b}\tilde{W}_i$ occurs via the exchange of $\tilde{t}_L$, $\tilde{b}_L$, or $\tilde{t}_R$ squarks. In terms of their respective amplitudes $\mathcal{M}_1$, $\mathcal{M}_2$, and $\mathcal{M}_3$, the partial width for the decay is given by

$$\Gamma(\tilde{g}\to t\bar{b}\tilde{W}_i)=\frac{1}{(2\pi)^5}\frac{1}{2m_{\tilde{g}}}\left(\tfrac{1}{2}\mathcal{M}_{11}+\tfrac{1}{2}\mathcal{M}_{22}+\tfrac{1}{2}\mathcal{M}_{33}\right.$$
$$\left.+\tfrac{1}{2}\mathcal{M}_{12}+\tfrac{1}{2}\mathcal{M}_{13}+\tfrac{1}{2}\mathcal{M}_{23}\right)\ , \tag{A2}$$

where

$$\tfrac{1}{2}\mathcal{M}_{11}=\pi^2g_s^2|A^d_{\tilde{W}_i}|^2m_{\tilde{g}}\int\frac{dE_t\,p_tE_t(m_{\tilde{g}}^2+m_t^2-2m_{\tilde{g}}E_t-m^2_{\tilde{W}_i})^2}{(m_{\tilde{g}}^2+m_t^2-2m_{\tilde{g}}E_t-m^2_{\tilde{t}_L})^2(m_{\tilde{g}}^2+m_t^2-2m_{\tilde{g}}E_t)}\ , \tag{A3a}$$

$$\tfrac{1}{2}\mathcal{M}_{22}=2\pi^2g_s^2m_{\tilde{g}}\int dE_{\bar{b}}\,E_{\bar{b}}^2\lambda^{1/2}(m_{\tilde{g}}^2-2m_{\tilde{g}}E_{\bar{b}},m^2_{\tilde{W}_i},m_t^2)$$
$$\times\frac{\frac{1}{2}(|A^u_{\tilde{W}_i}|^2+B^2_{\tilde{W}_i})(m_{\tilde{g}}^2-m_t^2-2m_{\tilde{g}}E_{\bar{b}}-m^2_{\tilde{W}_i})-2\,\text{Re}(iA^u_{\tilde{W}_i}B_{\tilde{W}_i}m_{\tilde{W}_i}m_t)}{(m_{\tilde{g}}^2-2m_{\tilde{g}}E_{\bar{b}}-m^2_{\tilde{b}_L})^2(m_{\tilde{g}}^2-2m_{\tilde{g}}E_{\bar{b}})}\ , \tag{A3b}$$

$$\tfrac{1}{2}\mathcal{M}_{33}=\pi^2 g_s^2 B_{\tilde{W}_i}^2 m_{\tilde{g}} \int \frac{dE_t\, p_t E_t (m_{\tilde{g}}^2+m_t^2-2m_{\tilde{g}}E_t-m_{\tilde{W}_i}^2)^2}{(m_{\tilde{g}}^2+m_t^2-2m_{\tilde{g}}E_t-m_{\tilde{t}_R}^2)^2(m_{\tilde{g}}^2+m_t^2-2m_{\tilde{g}}E_t)} , \tag{A3c}$$

$$\begin{aligned}\tfrac{1}{2}\mathcal{M}_{12}=\pi^2 g_s^2(-1)^{\theta_{\tilde{g}}} m_{\tilde{g}} \Bigg[& \mathrm{Re}(A_{\tilde{W}_i}^{d*} A_{\tilde{W}_i}^{u*}) m_{\tilde{W}_i} \int \frac{dE_t}{m_{\tilde{g}}^2+m_t^2-2m_{\tilde{g}}E_t-m_{\tilde{t}_L}^2} \\ & \times \left[E_{\bar{b}}(\max)-E_{\bar{b}}(\min)-\frac{m_{\tilde{b}_L}^2+m_t^2-2m_{\tilde{g}}E_t-m_{\tilde{W}_i}^2}{2m_{\tilde{g}}}\ln X \right] \\ & - B_{\tilde{W}_i}\,\mathrm{Re}(iA_{\tilde{W}_i}^{d*}) m_t \frac{1}{2m_{\tilde{g}}} \int dE_t \frac{m_{\tilde{g}}^2+m_t^2-2m_{\tilde{g}}E_t-m_{\tilde{W}_i}^2}{m_{\tilde{g}}^2+m_t^2-2m_{\tilde{g}}E_t-m_{\tilde{t}_L}^2}\ln X \Bigg] ,\end{aligned} \tag{A3d}$$

$$\begin{aligned}\tfrac{1}{2}\mathcal{M}_{23}=-\frac{\pi^2}{2} g_s^2 B_{\tilde{W}_i} \int \frac{dE_t}{m_{\tilde{g}}^2+m_t^2-2m_{\tilde{g}}E_t-m_{\tilde{t}_R}^2} \Bigg[& m_{\tilde{g}} B_{\tilde{W}_i}(m_{\tilde{g}}^2+m_t^2-2m_{\tilde{g}}E_t-m_{\tilde{W}_i}^2)\ln X \\ & - \frac{m_{\tilde{b}_L}^2-m_{\tilde{g}}^2}{m_{\tilde{g}}}[B_{\tilde{W}_i}(2E_t m_{\tilde{g}}-m_t^2-m_{\tilde{g}}^2)+\mathrm{Re}(iA_{\tilde{W}_i}^{u*}) m_{\tilde{W}_i} m_t]\ln X \\ & + [B_{\tilde{W}_i}(4E_t m_{\tilde{g}}-2m_t^2-2m_{\tilde{g}}^2)+2\,\mathrm{Re}(iA_{\tilde{W}_i}^{u*}) m_{\tilde{W}_i} m_t] \\ & \times [E_{\bar{b}}(\max)-E_{\bar{b}}(\min)] \Bigg] ,\end{aligned} \tag{A3e}$$

and

$$\tfrac{1}{2}\mathcal{M}_{13}=2\pi^2(-1)^{\theta_{\tilde{g}}} g_s^2\,\mathrm{Re}(iA_{\tilde{W}_i}^{d*}) m_{\tilde{g}} m_t B_{\tilde{W}_i} \int \frac{dE_t (m_{\tilde{g}}^2+m_t^2-2m_{\tilde{g}}E_t-m_{\tilde{W}_i}^2)[E_{\bar{b}}(\max)-E_{\bar{b}}(\min)]}{(m_{\tilde{g}}^2+m_t^2-2m_{\tilde{g}}E_t-m_{\tilde{t}_R}^2)(m_{\tilde{g}}^2+m_t^2-2m_{\tilde{g}}E_t-m_{\tilde{t}_L}^2)} . \tag{A3f}$$

In all but (A3b), the limits of integration on E_t are from m_t to $(m_{\tilde{g}}^2+m_t^2-m_{\tilde{W}_i}^2)/2m_{\tilde{g}}$, whereas

$$E_{\bar{b}}(\substack{\max\\\min}) = \frac{m_{\tilde{g}}^2-2m_{\tilde{g}}E_t+m_t^2-m_{\tilde{W}_i}^2}{2(m_{\tilde{g}}-E_t\mp p_t)}$$

and $p_t=\sqrt{E_t^2-m_t^2}$ and

$$X=\frac{m_{\tilde{b}_L}^2+2m_{\tilde{g}}E_{\bar{b}}(\max)-m_{\tilde{g}}^2}{m_{\tilde{b}_L}^2+2m_{\tilde{g}}E_{\bar{b}}(\min)-m_{\tilde{g}}^2} .$$

The limits of integration in Eq. (A3b) range from 0 to $[m_{\tilde{g}}^2-(m_t+m_{\tilde{W}_i})^2]/2m_{\tilde{g}}$.

The amplitude for the decay $\tilde{g}\to t\bar{t}\tilde{Z}_i$ has four contributions $\mathcal{M}_i$ $(i=1,\ldots,4)$ coming from the exchanges of $\bar{\tilde{t}}_L$, $\tilde{t}_L$, $\bar{\tilde{t}}_R$, nd $\tilde{t}_R$ squarks. In the limit of vanishing quark mass, the interference term between the amplitudes involving left $(\mathcal{M}_L=\mathcal{M}_1+\mathcal{M}_2)$ and right $(\mathcal{M}_R=\mathcal{M}_3+\mathcal{M}_4)$ squark exchange vanishes. The partial width for this decay is given by

$$\Gamma(\tilde{g}\to t\bar{t}\tilde{Z}_i)=\frac{1}{(2\pi)^5}\frac{1}{2m_{\tilde{g}}}(\tfrac{1}{2}\mathcal{M}_{LL}+\tfrac{1}{2}\mathcal{M}_{RR}+\tfrac{1}{2}\mathcal{M}_{13}+\tfrac{1}{2}\mathcal{M}_{14}+\tfrac{1}{2}\mathcal{M}_{23}+\tfrac{1}{2}\mathcal{M}_{24}) , \tag{A4}$$

with

$$\begin{aligned}\tfrac{1}{2}\mathcal{M}_{LL}=2g_s^2 \Bigg\{ & (|A_{\tilde{Z}_i}^t|^2+f_t^2 v_1^{(i)2})\psi(m_{\tilde{g}},m_{\tilde{t}_L},m_{\tilde{Z}_i}) - 4m_t m_{\tilde{Z}_i}(-1)^{\theta_i} A_{\tilde{Z}_i}^{\tilde{t}} f_t v_1^{(i)} \chi(m_{\tilde{g}},m_{\tilde{t}_L}) \\ & + (-1)^{\theta_{\tilde{g}}} m_{\tilde{g}} \Bigg[(-1)^{\theta_i} m_{\tilde{Z}_i} \Bigg(|A_{\tilde{Z}_i}^t|^2 \frac{1}{m_{\tilde{g}} m_{\tilde{Z}_i}} \phi(m_{\tilde{g}},m_{\tilde{t}_L},m_{\tilde{Z}_i}) + f_t^2 v_1^{(i)2} m_t^2 \rho(m_{\tilde{g}},m_{\tilde{t}_L}) \Bigg) \\ & + A_{\tilde{Z}_i}^{\tilde{t}} f_t v_1^{(i)} m_t [\xi(m_{\tilde{g}},m_{\tilde{t}_L},m_{\tilde{t}_L}) - m_{\tilde{Z}_i}^2 \rho(m_{\tilde{g}},m_{\tilde{t}_L})] \Bigg] \Bigg\} ,\end{aligned} \tag{A5a}$$

$$\tfrac{1}{2}\mathcal{M}_{RR}=\tfrac{1}{2}\mathcal{M}_{LL},\ \text{with}\ A^{\tilde{t}}_{\tilde{Z}_i}\to -B^{\tilde{t}}_{\tilde{Z}_i},\ |A^{t}_{\tilde{Z}_i}|^2\to|B^{t}_{\tilde{Z}_i}|^2,\ \text{and}\ m_{\tilde{t}_L}\to m_{\tilde{t}_R}\ , \tag{A5b}$$

$$\tfrac{1}{2}\mathcal{M}_{13}=\tfrac{1}{2}\mathcal{M}_{24}=4m_{\tilde{g}}m_t g_s^2(-1)^{\theta_{\tilde{g}}}\{[(-1)^{\theta_i+1}A^{\tilde{t}}_{\tilde{Z}_i}B^{\tilde{t}}_{\tilde{Z}_i}+f_t^2 v_1^{(i)2}(-1)^{\theta_i}]m_t m_{\tilde{Z}_i}\zeta(m_{\tilde{g}},m_{\tilde{t}_L},m_{\tilde{t}_R})$$
$$-f_t v_1^{(i)}(A^{\tilde{t}}_{\tilde{Z}_i}-B^{\tilde{t}}_{\tilde{Z}_i})X(m_{\tilde{g}},m_{\tilde{t}_L},m_{\tilde{t}_R})\}\ , \tag{A5c}$$

and

$$\tfrac{1}{2}\mathcal{M}_{14}=\tfrac{1}{2}\mathcal{M}_{23}=2g_s^2\{f_t^2 v_1^{(i)2}Y(m_{\tilde{g}},m_{\tilde{t}_L},m_{\tilde{t}_R})-A^{\tilde{t}}_{\tilde{Z}_i}B^{\tilde{t}}_{\tilde{Z}_i}m_t^2\xi(m_{\tilde{g}},m_{\tilde{t}_L},m_{\tilde{t}_R})$$
$$+f_t v_1^{(i)}m_t m_{\tilde{Z}_i}[(-1)^{\theta_i+1}A^{\tilde{t}}_{\tilde{Z}_i}\chi'(m_{\tilde{g}},m_{\tilde{t}_R},m_{\tilde{t}_L})+(-1)^{\theta_i}B^{\tilde{t}}_{\tilde{Z}_i}\chi'(m_{\tilde{g}},m_{\tilde{t}_L},m_{\tilde{t}_R})]\}\ . \tag{A5d}$$

The functions appearing above are defined as

$$\psi(m_{\tilde{g}},m_{\tilde{t}},m_{\tilde{Z}})=\pi^2 m_{\tilde{g}}\int dE_t p_t E_t\frac{m_{\tilde{g}}^2-m_{\tilde{Z}}^2-2m_{\tilde{g}}E_t}{(m_{\tilde{g}}^2+m_t^2-2m_{\tilde{g}}E_t-m_t^2)^2}\frac{\lambda^{1/2}(m_{\tilde{g}}^2+m_t^2-2m_{\tilde{g}}E_t,m_{\tilde{Z}}^2,m_t^2)}{m_{\tilde{g}}^2+m_t^2-2m_{\tilde{g}}E_t}\ , \tag{A6a}$$

$$\phi(m_{\tilde{g}},m_{\tilde{t}},m_{\tilde{Z}})=\tfrac{1}{2}\pi^2 m_{\tilde{g}}m_{\tilde{Z}}\int\frac{dE_t}{m_{\tilde{g}}^2+m_t^2-2m_{\tilde{g}}E_t-m_{\tilde{t}}^2}$$
$$\times\left[-[E_{\tilde{t}}(\max)-E_{\tilde{t}}(\min)]-\frac{m_{\tilde{Z}}^2-m_t^2+2m_{\tilde{g}}E_t-m_{\tilde{t}}^2}{2m_{\tilde{g}}}\ln Z(m_{\tilde{t}})\right]\ , \tag{A6b}$$

$$\chi(m_{\tilde{g}},m_{\tilde{t}})=\pi^2 m_{\tilde{g}}\int\frac{dE_t p_t E_t}{m_{\tilde{g}}^2+m_t^2-2m_{\tilde{g}}E_t}\frac{\lambda^{1/2}(m_{\tilde{g}}^2+m_t^2-2m_{\tilde{g}}E_t,m_{\tilde{Z}}^2,m_t^2)}{(m_{\tilde{g}}^2+m_t^2-2m_{\tilde{g}}E_t-m_{\tilde{t}}^2)^2}\ , \tag{A6c}$$

$$\xi(m_{\tilde{g}},m_{\tilde{t}_1},m_{\tilde{t}_2})=\tfrac{1}{2}\pi^2\int\frac{dE_t}{m_{\tilde{g}}^2+m_t^2-2m_{\tilde{g}}E_t-m_{\tilde{t}_1}^2}$$
$$\times\left[[E_{\tilde{t}}(\max)-E_{\tilde{t}}(\min)]-\frac{m_{\tilde{g}}^2-m_t^2-2m_{\tilde{g}}E_t+m_{\tilde{t}_2}^2}{2m_{\tilde{g}}}\ln Z(m_{\tilde{t}_2})\right]\ , \tag{A6d}$$

$$\rho(m_{\tilde{g}},m_{\tilde{t}})=-\frac{\pi^2}{2m_{\tilde{g}}}\int\frac{dE_t}{m_{\tilde{g}}^2+m_t^2-2m_{\tilde{g}}E_t-m_{\tilde{t}}^2}\ln Z(m_{\tilde{t}})\ , \tag{A6e}$$

$$\zeta(m_{\tilde{g}},m_{\tilde{t}_1},m_{\tilde{t}_2})=\pi^2\int\frac{dE_t[E_{\tilde{t}}(\max)-E_{\tilde{t}}(\min)]}{(m_{\tilde{g}}^2+m_t^2-2m_{\tilde{g}}E_t-m_{\tilde{t}_1}^2)(m_{\tilde{g}}^2+m_t^2-2m_{\tilde{g}}E_t-m_{\tilde{t}_2}^2)}\ , \tag{A6f}$$

$$X(m_{\tilde{g}},m_{\tilde{t}_1},m_{\tilde{t}_2})=\frac{\pi^2}{2}\int dE_t p_t\frac{m_{\tilde{g}}^2-m_{\tilde{Z}}^2-2m_{\tilde{g}}E_t}{m_{\tilde{g}}^2+m_t^2-2m_{\tilde{g}}E_t}\frac{\lambda^{1/2}(m_{\tilde{g}}^2+m_t^2-2m_{\tilde{g}}E_t,m_{\tilde{Z}}^2,m_t^2)}{(m_{\tilde{g}}^2+m_t^2-2m_{\tilde{g}}E_t-m_{\tilde{t}_1}^2)(m_{\tilde{g}}^2+m_t^2-2m_{\tilde{g}}E_t-m_{\tilde{t}_2}^2)}\ , \tag{A6g}$$

$$Y(m_{\tilde{g}},m_{\tilde{t}_1},m_{\tilde{t}_2})=\frac{\pi^2}{2}\int\frac{dE_t}{m_{\tilde{g}}^2+m_t^2-2m_{\tilde{g}}E_t-m_{\tilde{t}_1}^2}$$
$$\times\left[[E_{\tilde{t}}(\max)-E_{\tilde{t}}(\min)](m_{\tilde{g}}^2+m_t^2-2m_{\tilde{g}}E_t)\right.$$
$$\left.-\frac{1}{2m_{\tilde{g}}}(m_{\tilde{g}}^2m_{\tilde{Z}}^2-m_{\tilde{g}}^2m_{\tilde{t}_2}^2+m_t^4+2m_{\tilde{g}}E_t m_{\tilde{t}_2}^2-m_{\tilde{t}_2}^2m_t^2)\ln Z(m_{\tilde{t}_2})\right]\ , \tag{A6h}$$

and

$$\chi'(m_{\tilde{g}},m_{\tilde{t}_1},m_{\tilde{t}_2})--=\frac{\pi^2}{2}\int\frac{dE_t E_t}{m_{\tilde{g}}^2+m_t^2-2m_{\tilde{g}}E_t-m_{\tilde{t}_2}^2}\ln Z(m_{\tilde{t}_1})\ . \tag{A6i}$$

In Eqs. (A6), the limits of integration on E_t range from m_t to $(m_{\tilde{g}}^2-2m_t m_{\tilde{Z}_i}-m_{\tilde{Z}_i}^2)/2m_{\tilde{g}}$, and

$$Z(m)=\frac{m_{\tilde{g}}^2+m_t^2-2m_{\tilde{g}}E_{\bar{t}}(\max)-m^2}{m_{\tilde{g}}^2+m_t^2-2m_{\tilde{g}}E_{\bar{t}}(\min)-m^2} ,$$

and

$$E_{\bar{t}}(\substack{\max\\\min})=\frac{\zeta(m_{\tilde{g}}-E_t)\pm[p_t^2\zeta^2-4p_t^2m_t^2(m_{\tilde{g}}^2+m_t^2-2m_{\tilde{g}}E_t)]^{1/2}}{2(m_{\tilde{g}}^2+m_t^2-2m_{\tilde{g}}E_t)} ,$$

where $\zeta=2m_t^2+m_{\tilde{g}}^2-m_{\tilde{Z}_i}^2-2m_{\tilde{g}}E_t$ and $A_{\tilde{Z}_i}^{\tilde{t}}$ and $B_{\tilde{Z}_i}^{\tilde{t}}$ are as in Ref. [15]. Finally, the function λ that appears in Eqs. (A3) and (A6) is given by $\lambda(x,y,z)=x^2+y^2+z^2-2xy-2yz-2xz$.

[1] See, e.g., F. Dydak, in *Proceedings of the Twenty Fifth International Conference in High Energy Physics,* Singapore, 1990, edited by K. K. Phua and Y. Yamaguchi (World Scientific, Singapore, 1991).

[2] S. Pakvasa, D. P. Roy, and S. Uma-Shankar, Phys. Rev. D **42**, 3160 (1990).

[3] D. Dicus and V. Mathur, Phys. Rev. D **7**, 3111 (1973); B. Lee, C. Quigg, and H. B. Thacker, *ibid.* **16**, 1519 (1977).

[4] E. Gildener, Phys. Rev. D **14**, 1667 (1976).

[5] For reviews of supersymmetry and the minimal model, see H. P. Nilles, Phys. Rep. C **110**, 1 (1984); P. Nath, R. Arnowitt, and A. Chamseddine, in *Applied N=1 Supergravity,* ICTP Series in Theoretical Physics (World Scientific, Singapore, 1984), Vol. I; H. Haber and G. Kane, Phys. Rep. **117**, 75 (1985); X. Tata, in *The Standard Model and Beyond,* edited by J. E. Kim (World Scientific, Singapore 1991), p. 379.

[6] J. Gunion and H. Haber, Nucl. Phys. **B272**, 1 (1986).

[7] S. Wolfram, Phys. Lett. **82B**, 65 (1979); C. B. Dover, T. Gaisser, and G. Stiegman, Phys. Rev. Lett. **42**, 1117 (1979).

[8] P. F. Smith *et al.*, Nucl. Phys. **B149**, 525 (1979); **B206**, 333 (1982); E. Normal *et al.*, Phys. Rev. Lett. **58**, 1403 (1987).

[9] H. Baer, M. Drees, and X. Tata, Phys. Rev. D **41**, 3414 (1990); L. Krauss, Phys. Rev. Lett. **64**, 999 (1990).

[10] H. Baer, J. Ellis, G. Gelmini, D. Nanopoulos, and X. Tata, Phys. Lett. **161B**, 175 (1985); G. Gamberini, Z. Phys. C **30**, 605 (1986).

[11] H. Baer, V. Barger, D. Karatas, and X. Tata, Phys. Rev. D **36**, 96 (1987).

[12] R. Barnett, J. Gunion, and H. Haber, Phys. Rev. D **37**, 1892 (1988).

[13] H. Baer, M. Drees, D. Karatas, and X. Tata, in *Experiments, Detectors and Experimental Areas for the Supercollider,* Proceedings of the Workshop, Berkeley, California, 1987, edited by R. Donaldson and M. Gilchriese (World Scientific, Singapore, 1988), p. 210.

[14] A. Bartl, W. Majerotto, B. Mosslacher, N. Oshimo, and S. Stippel, Phys. Rev. D **43**, 2214 (1991).

[15] H. Baer, X. Tata, and J. Woodside, Phys. Rev. D **42**, 1568 (1990).

[16] CDF Collaboration, F. Abe *et al.*, Phys. Rev. D **43**, 664 (1991); A. Barbaro-Galtieri, presented at the Snowmass Workshop, 1990 (unpublished).

[17] J. F. Gunion and H. Haber, Phys. Rev. D **37**, 2515 (1988); H. Baer, A. Bartl, D. Karatas, W. Majerotto, and X. Tata, Int. J. Mod. Phys. A **4**, 4111 (1989).

[18] K. Hikasa and M. Kobayashi, Phys. Rev. D **36**, 724 (1987); I. Bigi and S. Rudaz, Phys. Lett. **153B**, 335 (1985); H. Baer, M. Drees, R. Godbole, J. Gunion, and X. Tata, Phys. Rev. D **44**, 725 (1991).

[19] H. Baer *et al.*, in *Research Directions for the Decade,* Proceedings of the Workshop, Snowmass, Colorado, 1990, edited by E. L. Berger and J. Butler (World Scientific, Singapore, 1991).

[20] M. Barnett, J. Gunion, and H. Haber, in *High Energy Physics in the 1990's,* edited by S. Jensen (World Scientific, Singapore, 1989), p. 230.

[21] H. Baer, X. Tata, and J. Woodside, Phys. Rev. D **42**, 1450 (1990).

[22] R. Barnett *et al.*, in *Experiments, Detectors and Experimental Areas for the Supercollider* [13], p. 178.

[23] R. M. Barnett and A. White, in *Research Directions for the Decade* [19].

[24] V. Fonseca, S. Kahn, M. Murtaugh, and F. Paige, in *Research Directions for the Decade* [19].

[25] C. Albajar *et al.*, in *Proceedings of the ECFA Large Hadron Collider Workshop,* Aachen, Germany, 1990, edited by G. Jarlskog and D. Rein (CERN Report No. 90-10, Geneva, Switzerland, 1990), Vol. II, p. 621.

[26] PYTHIA, H. Bengtsson and T. Sjostrand, Comput. Phys. Commun. **46**, 43 (1987).

[27] V. Barger, A. Stange, and R. Phillips, Phys. Rev. D **44**, 1987 (1991).

[28] V. Barger, T. Han, and H. Pi, Phys. Rev. D **41**, 824 (1990).

[29] H. Komatsu and H. Kubo, Nucl. Phys. **B263**, 265 (1986); H. Haber and D. Wyler, *ibid.* **B323**, 267 (1989).

[30] As discussed by Haber and Wyler [29], the radiative decays of the neutralino are not very important unless either both neutralinos are Higgsinolike, or (in the case of light neutralinos) one is a light photino and the other a Higgsino.

[31] ISAJET, F. Paige and S. Protopopescu, in *Supercollider Physics,* Proceedings of the Topical Conference, Eugene, Oregon, 1985, edited by D. Soper (World Scientific, Singapore, 1986), p. 41.

[32] Particle Data Group, J. Hernández *et al.*, Phys. Lett. B **239**, 1 (1990); B. Bambah *et al.*, in *Z Physics at LEP 1,* Proceedings of the Workshop, Geneva, Switzerland, 1989, edited by G. Altarelli, R. Kleiss, and C. Verzegnassi (CERN Yellow Report No. 89-08, Geneva, 1989), Vol. 3, p. 143.

[33] JETSET 7.2, T. Sjostrand, Comput. Phys. Commun. **39**, 347 (1986).
[34] H. Baer, V. Barger, H. Goldberg, and J. Ohnemus, Phys. Rev. D **38**, 3467 (1988).
[35] Z. Kunszt, Nucl. Phys. **B247**, 339 (1984).
[36] A 20 000 event run of SUSYSM on a Vax 3100 M76 takes about 10 h of CPU time.
[37] P. Langacker, Phys. Rev. Lett. **63**, 1920 (1989); J. Ellis and G. Fogli, Phys. Lett. B **249**, 543 (1990); V. Barger, J. Hewett, and T. Rizzo, Phys. Rev. Lett. **65**, 1313 (1990).
[38] E. Eichten, I. Hinchliffe, K. Lane, and C. Quigg, Rev. Mod. Phys. **56**, 579 (1984).
[39] Because of a programming error, the $\not{E}_T$ cross sections shown in Fig. 9 of Ref. [19] were too small by a factor of about 3.
[40] U. Ellwanger, Phys. Lett. **141B**, 435 (1984).
[41] Y. Okada, M. Yamaguchi, and T. Yanagida, Phys. Lett. B **262**, 54 (1991); Prog. Theor. Phys. **85**, 1 (1991); H. Haber and R. Hempfling, Phys. Rev. Lett. **66**, 1815 (1991); J. Ellis, G. Ridolfi, and F. Zwirner, Phys. Lett. B **257**, 33 (1991).
[42] ALEPH Collaboration, D. Decamp *et al.*, Phys. Lett. B **241**, 141 (1990); **265**, 475 (1991); P. Abreu *et al.*, *ibid.* **245**, 276 (1990); L3 Collaboration, B. Adeva *et al.*, *ibid.* **251**, 311 (1990); OPAL Collaboration, M. Akrawy *et al.*, Z. Phys. C **49**, 1 (1991).
[43] M. Chanowitz and M. Gaillard, Nucl. Phys. **B261**, 369 (1985); M. Chanowitz and M. Golden, Phys. Rev. Lett. **61**, 1053 (1988); D. Dicus and R. Vega, Nucl. Phys. **B329**, 533 (1990).
[44] D. Dicus and R. Vega, Phys. Lett. B **217**, 194 (1989).
[45] We are grateful to R. Vega for providing us the cross sections for inclusive l^+l^+ production that we use to obtain the entries in Tables III and IV for backgrounds from $W^{\pm}W^{\pm}$ production.
[46] V. Barger and T. Han, Phys. Lett. B **212**, 117 (1988).
[47] J. Gunion and Z. Kunszt, Phys. Lett. **159B**, 167 (1985); Phys. Lett. B **176**, 477 (1986); H. Baer, V. Barger, H. Goldberg, and R. Phillips, Phys. Rev. D **37**, 3152 (1988); R. Fletcher, F. Halzen, and C. Kim, Phys. Lett. B **209**, 351 (1988).
[48] B. Humpert, Phys. Lett. **135B**, 179 (1984).
[49] F. Halzen, P. Hoyer, and W. Stirling, Phys. Lett. B **188**, 375 (1987).
[50] J. Freeman (private communication).
[51] D. Dicus and S. Willenbrock, Phys. Rev. D **39**, 751 (1989).
[52] D. Dicus and C. Kao, Phys. Rev. D **41**, 832 (1990).
[53] E. Witten, Nucl. Phys. **B185**, 513 (1981); R. Kaul, Phys. Lett. **109B**, 19 (1981); N. Sakai, Z. Phys. C **11**, 153 (1981); S. Dimopoulos and H. Georgi, Nucl. Phys. **B193**, 150 (1981).
[54] U. Amaldi, W. de Boer, and H. Furstenau, Phys. Lett. B **260**, 447 (1991).